

# Expansion, Topology and Entropy

Gerd Pommerenke

Email: gerdpommerenke@arcor.de

## Abstract

Object of this work is, to determine, if objects observed more distant are moving away faster than less distant ones. The escape velocity  $Hr$  is defined by the HUBBLE-Parameter  $H$ , locally  $H_0$ , which is proportional to the reciprocol of the age  $T$ . The calculations are based on the model published in viXra:1310.0189. The idea stems from Cornelius LANCZOS, outlined at a lecture on the occasion of the Einstein-Symposium 1965 in Berlin. The model defines the expansion of the universe as a consequence of the existence of a metric wave field. That field also should be the reason for all relativistic effects, both SR and GR. In the context of this work the propagation function of that wave field is determined. Its phase rate is equal to the reciprocal of PLANCK's smallest increment  $r_0$ . Even the other PLANCK-units set up the basis of the model being functions of space and time. With it, the model leads to a quantization of the universe into single line-elements with the size of  $r_0$ . Thus, a kind of finite-element-method becomes possible, at which point the single elements are explicitly defined by the wave function. As per definition, objects in the free fall, aren't moving either with respect to the metrics and are carried-with during expansion. With the help of the propagation function it's possible to calculate the HUBBLE-Parameter  $H$  even for greater distances. Furthermore the entropy of the universe as a whole is determined considering the special topology of the universe. German version available in viXra. „Expansion, Topologie und Entropie”

2<sup>nd</sup> Edition Augsburg © 2024



## 1. Preamble

Object of this work is, to determine, if objects observed more distant than  $0.01R$  (world radius) are moving away faster than less distant ones. Mostly astronomers and cosmologists are interested in that question. The escape velocity  $Hr$  is just defined by the HUBBLE-Parameter  $H$ , locally  $H_0$ , which is proportional to the reciprocal of the age  $T$ . Hence it's not about a constant either. Therefore I'm intentionally using the word parameter. Furthermore should be examined, if it's possible, to calculate the entropy of the universe as a whole, and in which regard we have to consider its special topology (4D).

The calculations are based on the model published in [1] and [10]. The idea stems from Cornelius LANCZOS [2], outlined at a lecture on the occasion of the Einstein-Symposium 1965 in Berlin. This lecture is also prefixed to [1]. The model defines the expansion of the universe as a consequence of the existence of a four-legged wave field. That field also should be the reason for all relativistic effects, both SR and GR. The temporal function of that field is based on the Hankel function, consisting of the sum of two Bessel functions ( $J_0$  and  $Y_0$ ). The special properties of the Bessel functions lead to an increase of wave length, defined by the distance between two zero-crossings. The propagation velocity  $c_M$  of the field depends on space and time being in the range between  $1.09 \cdot 10^{-22} \text{ms}^{-1}$  (nowadays) at the local observer up to  $0.851661c$  at the particle horizon.

That involves, that the wave length  $\lambda_0$  and the phase rate  $\beta_0$  of the propagation function are having different values. Its phase rate is equal to the reciprocal of PLANCK's smallest increment  $r_0$ . Even the other PLANCK-units set up the basis of the model being functions of space and time. In the distance  $r_0$  in the form of a cubic face-centered space-lattice (fc) particular vortices are collocated. LANCZOS called them „MINKOWSKIAN line elements, which are only approximately MINKOWSKIAN“, here abbreviated as MLE. Thus it's rather about a physical object and not about that, the MINKOWSKIAN line element is actually defined. I nominated the whole wave field as metric wave field (metrics).

With it, the model leads to a quantization of the universe into single line-elements with the size of  $r_0$ . Thus, a kind of *finite-element-method* becomes possible, at which point the single elements are explicitly defined by the wave function. The wave length  $\lambda_0$  and  $r_0$  are increasing over time. As per definition, objects in the free fall, aren't moving either with respect to the metrics and are carried-with during expansion. With the help of the propagation function it's possible to calculate the HUBBLE-Parameter  $H$  even for greater distances. Farther away we just observe a greater local  $H_0$ , because  $H$  was greater in the old days. Summarized, with greater distance even a greater  $H$  should turn out, which the calculation confirms.

Because the entropy of wave fields can be calculated, it will be determined too. But we have to consider special circumstances at this point. It allows a foresight into the far future of our universe. Finally, the work deals with the different kinds of distance vectors and the question is answered, why vectors greater than  $cT$  are possible.

A special feature of the model is, that the so called *subspace*, that's the space, the metric wave field propagates in, disposes of a third property among  $\mu_0$  and  $\epsilon_0$ . That's the specific conductivity  $\kappa_0$  in the size of  $1.23879 \cdot 10^{93} \text{Sm}^{-1}$ , the cause of expansion. Whether and how it doesn't lead to contradictions with the propagation of „normal“ EM-waves, is *not* subject of the work on hand. According to the model they propagate as overlaid interferences of the metric wave field. See [1] for more detailed information. There you will find even a special section dedicated to the unexpected results of the SN-1a-Cosmology-Experiment.

## 2. Fundamentals and hypotheses

Before we get to the actual calculation, it's necessary, to define certain base items of the model, mostly without derivation. You read about this in [10]. The PLANCK-units, furthermore the base items of the theoretical electro-technics play a very special role in this connection. For this reason, as usual there, I'm using the letter  $j$  instead of  $i$  or  $\mathfrak{i}$  as usual in mathematics.

### 2.1. Definition of base items

At first the base items of the theoretical electro-technics. They apply independently from the model (1). Beneath (2) the most important PLANCK-units are shown. The introduction of the specific conductivity of the vacuum turns out to be the *missing link* among each other and even to other values.

$$c = \frac{1}{\sqrt{\mu_0 \varepsilon_0}} \quad \left| \quad Z_0 = \sqrt{\frac{\mu_0}{\varepsilon_0}} = \sqrt{\frac{L_0}{C_0}} = \frac{\varphi_0}{q_0} = \frac{\mathbf{E}}{\mathbf{H}} \quad \left| \quad \begin{array}{l} L_0 = \mu_0 r_0 \quad C_0 = \varepsilon_0 r_0 \\ R_0 = 1/(\kappa_0 r_0) \end{array} \right. \quad (1)$$

$$r_0 = \sqrt{\frac{G\hbar}{c^3}} = \sqrt{\frac{2t}{\mu_0 \kappa_0}} \quad \left| \quad m_0 = \sqrt{\frac{\hbar c}{G}} = \frac{\mu_0 \kappa_0 \varphi_0^2}{Z_0} \quad \left| \quad \varphi_0 = \sqrt{\hbar Z_0} \quad q_0 = \sqrt{\hbar/Z_0} \quad (2)$$

One single line-element can be specified by the model of a lossy Schwingkreises mit oscillating circuit. One special property *of that model only* is, that the Q-factor of the circuit equals the phase angle  $2\omega_0 t$  of the Bessel function. It applies  $Q_0 = 2\omega_0 t$ . The value  $\omega_0$  corresponds to the PLANCK-frequency in this connection.

$$\omega_0 = \sqrt{\frac{c^5}{G\hbar}} = \sqrt{\frac{\kappa_0}{2\varepsilon_0 t}} = \frac{1}{\sqrt{L_0 C_0}} = \frac{c}{r_0} \quad \left| \quad t_0 = \sqrt{\frac{G\hbar}{c^5}} = \sqrt{\frac{\varepsilon_0 t}{2\kappa_0}} \quad (3)$$

$$Q_0 = 2\omega_0 t = \kappa_0 r_0 Z_0 = \frac{\hbar R_0}{\varphi_0^2} = \frac{R_0}{Z_0} = \left( \frac{c}{c_{M+v}} \right)^2 = \sqrt{\frac{2\kappa_0 t}{\varepsilon_0}} \quad (4)$$

$$H_0 = \frac{\dot{r}_0}{r_0} = \frac{1}{R_0 C_0} = \frac{\varepsilon_0}{\kappa_0} \frac{1}{L_0 C_0} = \frac{1}{\kappa_0 \mu_0 r_0^2} = \frac{\varepsilon_0 \omega_0^2}{\kappa_0} = \frac{1}{2T} = \frac{\omega_0}{Q_0} \quad (5)$$

The numeric value of  $Q_0$  according to table 1 is about  $7.5419 \cdot 10^{60}$  and depends on the real value of  $H_0$ . Except for the quantities of subspace  $\mu_0$ ,  $\varepsilon_0$ ,  $\kappa_0$  and  $c$  all other ones are functions of space, time and even of the velocity  $v$  with respect to the metric wave field. The reason is, that the spatiotemporal function of the metric wave field should emulate the relativistic effects. The GR-dependencies aren't furthermore considered here.

That makes the PLANCK units depend on the frame of reference, which is even defined by them. And all of them are bound by the phase angle  $Q_0$ . But the variations mostly cancel each other creating the impression, that the values are constant. Reference-frame-dependent values are marked with a swung dash e.g.  $\tilde{Q}_0$  being constants by character.

Still important are the values with a phase angle  $Q_1 = 1$ . They describe the conditions directly at the particle horizon. They are constants too, because they are defined only by quantities of subspace. Thus, they are mostly qualified for reference-frame-independent conversions of certain values, so-called couplings. An example is the conversion of the magnetic flux  $\varphi_1$  to the magnetic field strength  $H_1 = \varphi_1 / (\mu_0 r_1^2)$  as basis of a temporal function containing reference-frame-dependent elements ( $r_0$ ).  $r_1$  would be the so-called coupling-length then.

Expression (8) shows the relations to the PLANCK-units and to the values of the universe as a whole.

$$r_1 = \frac{1}{\kappa_0 Z_0} \quad \left| \quad M_1 = \mu_0 \kappa_0 \hbar \quad \right| \quad t_1 = \frac{1}{2} \frac{\varepsilon_0}{\kappa_0} \quad \left| \quad \omega_1 = \frac{\kappa_0}{\varepsilon_0} = \frac{1}{2t_1} \quad \right| \quad (6)$$

$$R = Q_0 r_0 = Q_0^2 r_1 \quad \left| \quad M_1 = Q_0 m_0 \quad \right| \quad T = Q_0 t_0 = Q_0^2 t_1 \quad \left| \quad \omega_1 = Q_0 \omega_0 = Q_0^2 H_0 \quad \right| \quad (7)$$

$$\varphi_1 = \sqrt{\hbar_1 Z_0} \quad \left| \quad q_1 = \sqrt{\hbar_1 / Z_0} \quad \right| \quad \hbar_1 = \hbar Q_0 \quad \left| \quad \kappa_0 = \frac{c^3}{\mu_0 G \hbar H_0} \quad \right| \quad (8)$$

The action quantum  $\hbar_1$  and  $\hat{\hbar}_1$  is not a quantity of subspace, but the initial action, our universe „got“ in the early beginning. That value is the only one „set-screw“, with which „one“ could exert influence on the future appearance of the universe. All other values are „hard-wired“ with  $Q_0$  depending on space and time. There is no „fine-tuning“ either. With expression (2) right-hand and (8) it's about an effective value, i.e.  $\hbar$ ,  $\varphi_0$  and  $q_0$  are temporal functions too. For section 3.2.1. still the definition of NEWTON's gravitational constant:

$$G = \frac{c^3}{\mu_0 \kappa_0 \hbar H} = \frac{2c^3 t}{\mu_0 \kappa_0 \hbar} = c^2 \frac{R}{M_1} = c^2 \frac{r_0}{m_0} \quad (868 [10])$$

## 2.2. Temporal function

We get the exact temporal function for the magnetic flux  $\varphi_0$  by solving the differential equation (9). It is based on a lossy oscillating circuit *with expansion*, i.e. the single components  $R_0$ ,  $L_0$  and  $C_0$  are changing with increasing  $r_0$ . Expression (9) mainly differs from a normal oscillating circuit without expansion, with harmonic solution by the factor before  $\varphi_0$ , 1 with expansion,  $\frac{1}{2}$  without.

$$\ddot{\varphi}_0 t + \dot{\varphi}_0 + \frac{1}{2} \frac{\kappa_0}{\varepsilon_0} \varphi_0 = 0 \quad (9)$$

In contrast to the expression without expansion there is no drop-down in the resonance frequency  $\omega_0$  with (9), normally caused by the influence of the loss-resistance  $R_0$ . But we obtain another as solution:

$$y = a_0 {}_0F_1(;1;-Bx) \quad \text{with} \quad a_0 = \hat{\varphi}_i / 2 \quad B = \frac{1}{2} \frac{\kappa_0}{\varepsilon_0} \quad x = t \quad (10)$$

According to [4] applies

$${}_0F_1(;b;x) = \Gamma(b)(jx)^{b-1} J_{b-1}(j2x^{\frac{1}{2}}) \quad \text{Hypergeometric function } {}_0F_1 \quad (11)$$

$J_n$  is the Bessel function of  $n^{\text{th}}$  order, thus

$${}_0F_1(;1;-Bx) = \Gamma(1)(jBx)^0 J_0(\sqrt{4Bx}) \quad (12)$$

$$y = a_0 J_0(\sqrt{4Bx}) \quad (13)$$

$$\varphi_0 = a_0 J_0\left(\sqrt{\frac{2\kappa_0 t}{\varepsilon_0}}\right) = a_0 J_0(Q_0) \quad (14)$$

Since it's about a differential equation of 2<sup>nd</sup> order and the grade of the Bessel function is integer, the general solution is:

$$\varphi_0 = \hat{\varphi}_i (c_1 J_0(2\omega_0 t) + c_2 Y_0(2\omega_0 t)) \quad (15)$$

The factors  $c_1$  and  $c_2$  may be imaginary or complex even here. According to [5] it's more favourable, if we consider both Hankel functions:

$$H_0^{(1)}(x) = J_0(x) + Y_0(x) \quad \text{and} \quad (16)$$

$$H_0^{(2)}(x) = J_0(x) - Y_0(x) \quad (17)$$

as linearly independent solutions composing the general solution

$$y(x) = c_1 H_0^{(1)}(x) + c_2 H_0^{(2)}(x) \quad (18)$$

with it. Then, the general solution (15) reads then:

$$\varphi_0 = \hat{\varphi}_i (H_0^{(1)}(2\omega_0 t) + H_0^{(2)}(2\omega_0 t)) \quad (19)$$

For our further examinations, we set  $c_1$  and  $c_2$  in (19) equal to 1 for the moment. Then we get as specific solution (20) and for approximation, envelope curve and effective value:

$$\varphi_0 = \hat{\varphi}_i J_0(2\omega_0 t) = \hat{\varphi}_i \operatorname{Re}(H_0^{(1)}(2\omega_0 t)) \quad \varphi_0 = \hat{\varphi}_i J_0\left(\sqrt{\frac{2\kappa_0 t}{\varepsilon_0}}\right) \quad (20)$$

$$\varphi_0 = \sqrt{\frac{2}{\pi}} \frac{1}{\sqrt{2\omega_0 t}} \cos\left(2\omega_0 t - \frac{\pi}{4}\right) \quad \text{Approximation} \quad (21)$$

$$\hat{\varphi}_0 = \sqrt{\frac{2}{\pi}} \frac{\hat{\varphi}_i}{\sqrt{2\omega_0 t}} \quad \text{Envelope curve} \quad (22)$$

$$\varphi_0 = \frac{\varphi_1}{\sqrt{2\omega_0 t}} \quad \varphi_0 \sim q_0 \sim Q_0^{-\frac{1}{2}} \quad \hbar = \varphi_0 q_0 \sim Q_0^{-1} \quad \text{Effective value} \quad (23)$$

The exact course of  $\varphi_0$  (20), as well as of the approximate function of the envelope curve (21) and of the effective value (22) is shown in figure 1. Also depicted are the original Bessel functions, which you can't see however, because they are completely covered by the approximation.

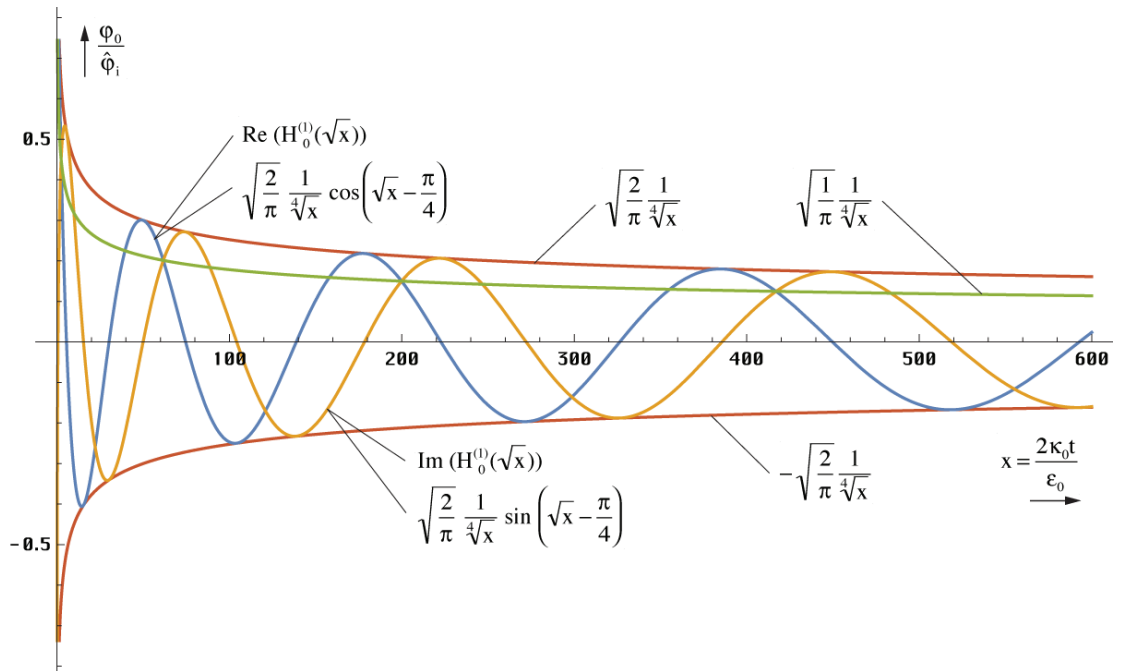


Figure 1  
Course of magnetic flux as well as of approximation- and envelope-functions across a greater time period

Thus, with greater arguments, no differences are statable, neither in the amplitude, nor in the phase. Most important for the quality of the approximation is the course in the striking distance of  $t=0$ . It is shown in figure 2 and it turns out to be very good until the particle horizon at  $Q_0=1$ . All data so far are summarized. See [1] for details and the exact derivation.

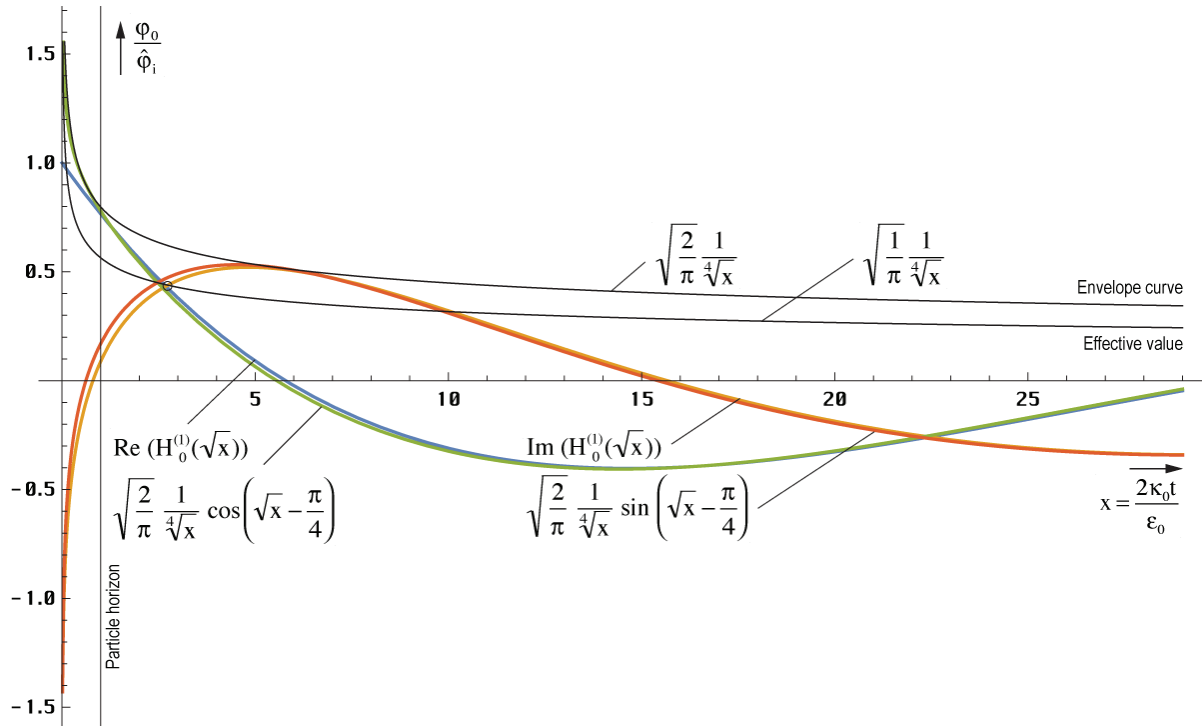


Figure 2  
Course of flux as well as of the approximate-  
and envelope-functions nearby the singularity

## 2.3. Propagation function

### 2.3.1. Exact solution

#### 2.3.1.1. Temporal function

In contrast to MAXWELL, which used the first term of the harmonic solution (108 [1])  $e^{i\omega t}$  as ansatz, we now choose the first term of expression (19), obtained as an independent solution of the differential equation (9). It's about the temporal function of the magnetic flux  $\varphi_0$  there, relating to one single MLE, from which the charge  $q_0$  can be derived. For the propagation function however we need the magnetic and electric field strength  $\mathbf{H}$  and  $\mathbf{E}$ . The relation:

$$\varphi = \int_A \mathbf{B} dA \quad \text{with } \mathbf{B} = \mu_0 \mathbf{H} \quad \text{leads to} \quad |\mathbf{H}| = \frac{\hat{\varphi}_0}{\mu_0 r_0^2} \quad (24)$$

Because of  $r_0$  indeed the right-hand expression depends on the frame of reference. Moreover we are rather looking for the starting value at  $T=0$ . The temporal function is just known. Hence, we must carry out a reference-frame-independent coupling only. The coupling-length  $r_k$  is not arbitrary in this case. Because the imaginary part of the Hankel function is coming from infinity, the starting value  $\varphi_0$  is defined at the point  $2\omega_0 t = Q_0 = 1$ . The coupling-length at this point is  $r_1$  as already predicted more above. This value is denominated as  $\mathbf{H}_1$  resp.  $\mathbf{E}_1$ . With respect to the fact, that (23) is an effective value, we obtain the following relations:

$$\mathbf{E}_1 = \frac{q_1}{\varepsilon_0 r_1^2} \sqrt{2} = \frac{1}{Z_0} \frac{\Phi_0}{\varepsilon_0 r_0^2} \sqrt{2} \quad \mathbf{H}_1 = \frac{\Phi_0}{\mu_0 r_0^2} \sqrt{2} \quad (25)$$

$$\underline{\mathbf{E}} = \mathbf{E}_1 H_0^{(1)}(2\omega_0 t) \quad \underline{\mathbf{H}} = \mathbf{H}_1 H_0^{(1)}(2\omega_0 t) \quad (26)$$

Here again, the real part of the vector corresponds to an orientation in y-, the imaginary one in z-direction, x is the propagation direction. As already stated, there is an analogy between the exponential function  $e^{j2\omega t}$  and the Hankel function. Both are transcendent complex functions and periodic resp. almost periodic. Of course, there is also a solution of the MAXWELL equations for (26). The detailed derivation can be read in [1] once again. Important is the complex wave propagation velocity  $\underline{c}$  and the field wave impedance  $\underline{Z}_F$ :

$$\underline{c} = \frac{c}{j\omega_0 t} \frac{1}{\sqrt{1 - \left( \frac{H_2^{(1)}(2\omega_0 t)}{H_0^{(1)}(2\omega_0 t)} \right)^2}} \quad \text{with} \quad \Theta = \frac{H_2^{(1)}(2\omega_0 t)}{H_0^{(1)}(2\omega_0 t)} \quad (27)$$

$$\underline{c} = \frac{c}{j\omega_0 t} \frac{1}{\sqrt{1 - \Theta^2}} \quad \underline{Z}_F = \frac{Z_0}{j\omega_0 t} \frac{1}{\sqrt{1 - \Theta^2}} \quad (28)$$

One can see, the propagation velocity tends to zero for greater t. The same applies even to the field wave impedance. We have to do with a quasi-stationary wave field (standing wave), which fulfils the requirements, made on a metrics, very well. The propagation velocity is complex again. A split into real- and imaginary part proves to be quite difficult, but it's mathematically possible. The solution for  $\underline{c}$  reads:

$$A = \frac{J_0(Q_0)J_2(Q_0) + Y_0(Q_0)Y_2(Q_0)}{J_0^2(Q_0) + Y_0^2(Q_0)} \quad \rho_0 = \frac{1}{2} \sqrt[4]{(1 - A^2 + B^2)^2 + (2AB)^2} \quad (29)$$

$$B = \frac{J_2(Q_0)Y_0(Q_0) - J_0(Q_0)Y_2(Q_0)}{J_0^2(Q_0) + Y_0^2(Q_0)} \quad \rho_0 = \frac{1}{2} \left| \sqrt{1 - \Theta^2} \right| \quad \theta = \frac{2AB}{1 - A^2 + B^2}$$

$$\frac{1}{\rho_0 Q_0} = \frac{c_M}{c} = \frac{1}{Q_0} \left| \frac{2}{\sqrt{1 - \Theta^2}} \right| \quad \text{RhoQ} = 2 / \# / \text{Abs}[\text{Sqrt}[1 - (\text{HankelH}[2, \#] / \text{HankelH}[0, \#])^2]] \& \quad (30)$$

$$\phi_0 = \frac{1}{2} \arctan \theta = \arg \left[ \frac{1}{\sqrt{1 - \Theta^2}} \right] - \frac{\pi}{2} \quad \text{PhiQ} = \text{Arg}[1 / \text{Sqrt}[1 - (\text{HankelH}[2, \#] / \text{HankelH}[0, \#])^2]] - \pi / 2 \&$$

An altogether quite complex expression turns out, that can still be simplified someway however (31). A starts at  $+\infty$  converging to  $-1$ . The course resembles the function  $1/A^2 - 1$  approximately, which cannot be used well as approximation however. B has a course like  $1/B^2$  and is converging to zero. The same is applied even to  $\theta$  then. The bracketed expression converges to 1 with it.  $1/\rho_0$  is the value-function converging to  $1/2\sqrt{2}$ .

$$\underline{c} = -\frac{2}{\rho_0} \frac{c}{2\omega_0 t} \left( \sin \frac{1}{2} \arctan \theta + j \sin \frac{1}{2} \arctan \theta \right) = \frac{2}{\rho_0} \frac{c}{2\omega_0 t} e^{-j \frac{1}{2} (\arctan \theta + \pi)} \quad (31)$$

Unfortunately (31) cannot be transformed into an expression similar to (179 [1]) with area-functions, so that the ambiguity of the arctan-function leads to a partially wrong result. We should better calculate with the following substitution therefore:

<sup>1</sup> For programming reasons, expression (29) with AB turns out a slightly different result than (27). In order to maximize accuracy, only function (27) is used to the calculation of values and graphics.



$$\arctan \theta = \arg \sqrt{1 - A^2 + B^2 + j2AB} \quad \arg \underline{c} = \frac{1}{2} \operatorname{arccot} \theta - \frac{\pi}{4} \quad (32)$$

While the real part of  $\underline{c}$  is defined as the velocity in propagation direction, the imaginary part can be interpreted as a velocity rectangular thereto. The appearance of an imaginary part in  $\underline{c}$  means also that there is an attenuation anywhere (refer to figure 4). A numerical handling of (27) even can be processed with »Mathematica« resulting in the course figured in figure 3. Since the Hankel functions, with larger arguments, can be expressed well by other analytic functions, we will declare approximate solutions later on.

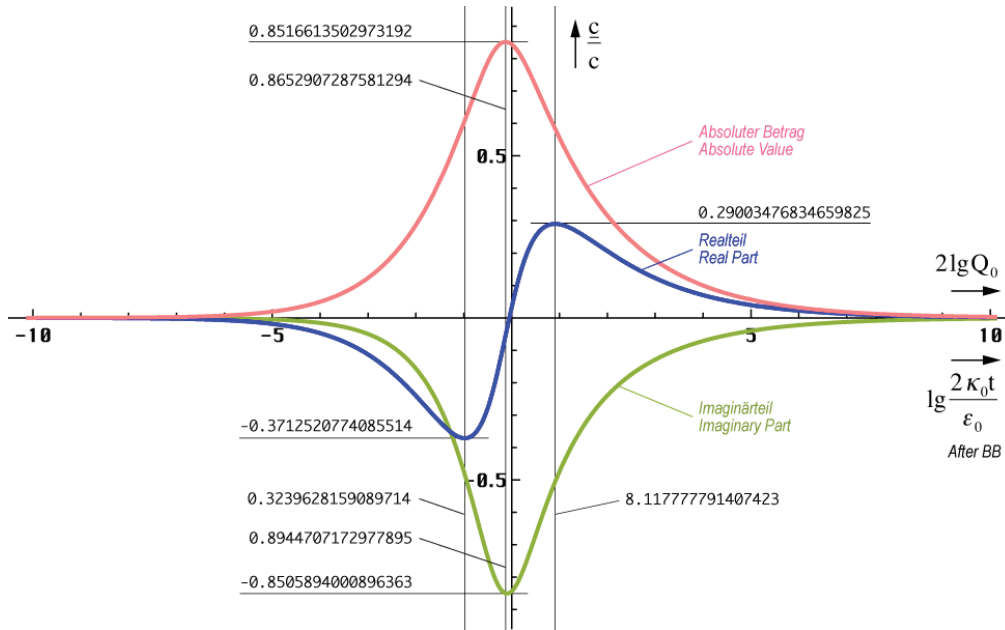


Figure 3  
Propagation-velocity  
in dependence on time (logarithmic time-scale)

With it, the world-radius (wave-front) of this model doesn't expand with  $c$  but with  $0.851661c$  only. That figures no violation of the SRT anyway. This means that wave sections that are emitted later virtually overtake the wave front. Since the ratio of real and imaginary part is different, it does not happen on the same path – rather, the wave fronts cross each other. However, a contradiction arises to the usual definition  $R/2=cT$  (Radiation Universe), which will be solved later on.

### 2.3.1.2. Propagation rate

To specify the propagation-function we need both, the temporal function and the propagation rate  $\gamma = \alpha + j\beta$ . The normal form of the propagation function is given by:

$$\underline{\mathbf{E}} = \mathbf{E} e^{j\omega \left( t - \frac{x}{\underline{c}} \right)} = \mathbf{E} e^{j\omega t - \gamma x} = \mathbf{E} e^{j(\omega t + j\beta x)} \quad (33)$$

In contrast to (33) the argument in the expansion case is real. Strictly speaking, it's not the Hankel function but the modified Hankel function  $M_0^{(2)} = I_0(z) - jK_0(z)$  what's the equivalent to the exponential function. It applies  $I_0(z) = J_0(jz)$  but only for purely imaginary arguments. With complex arguments, the real part cannot be placed as a factor in front of the Hankel function in the form of  $e^a \times e^{jb}$ , as usual with exponential functions, since the power laws don't apply to Hankel functions. This is only possible for larger arguments  $z$ . However, the modified Hankel function is generally not used. Therefore, we use for the base the "ordinary" Hankel function adapting the propagation-function accordingly. To avoid contra-dictions with

the classic definition of propagation rate – real-part equals the attenuation rate, imaginary-part equals the phase-rate – the propagation-function should read as follows then (analogously for  $\underline{\mathbf{H}}$ ):

$$\underline{\mathbf{E}} = \mathbf{E} H_0^{(1)} \left( 2\omega_0 \left( t - \frac{x}{\underline{c}} \right) \right) = \mathbf{E} H_0^{(1)} (2\omega_0 t - j\underline{\gamma}x) \quad (34)$$

This is not quite the classic expression for a propagation-function. Attention should be paid to the factor 2 which can be assigned both to the frequency, as well as the time-constant. With the definition of propagation rate  $\underline{\gamma} = \alpha + j\beta$  it obviously belongs to the frequency since  $\underline{\gamma}$  depends on phase velocity  $dx/dt$ , but not on the half of  $dx/(2dt)$ . By equating both arguments of (34) one gets then:

$$\underline{\gamma} = -\frac{2\omega_0}{\underline{c}} = j\kappa_0 Z_0 \sqrt{1 - \Theta^2} \quad (35)$$

From (31) the reciprocal of  $\underline{c}$  can be determined very easily. Then we get for  $\underline{\gamma}$ :

$$\frac{1}{\underline{c}} = -\frac{\omega_0 t \rho_0}{c} \left( \cos \frac{1}{2} \arctan \theta - j \sin \frac{1}{2} \arctan \theta \right) \quad (36)$$

$$\underline{\gamma} = \alpha + j\beta = -2\omega_0 / \underline{c} = \frac{2\omega_0^2 t \rho_0}{c} \left( \cos \frac{1}{2} \arctan \theta - j \sin \frac{1}{2} \arctan \theta \right) \quad (37)$$

$$\underline{\gamma} = \rho_0 \kappa_0 Z_0 \left( \cos \frac{1}{2} \arctan \theta - j \sin \frac{1}{2} \arctan \theta \right) \quad (38)$$

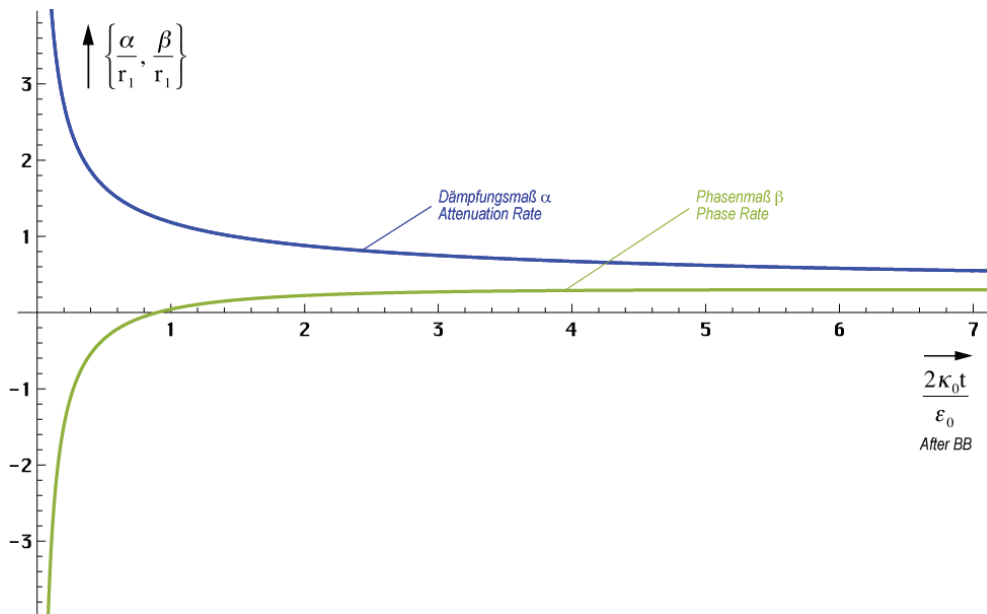


Figure 4  
Phase-rate and attenuation rate  
in dependence on time (linear scale)

With accurate contemplation one recognizes that  $\alpha$  and  $\beta$ , evaluated by its action, are exchanged in fact ( $\alpha$  = phase-rate,  $\beta$  = attenuation rate). This is caused thereby that a rotation of about  $90^\circ$  ( $j$ ) occurs during propagation (figure 7).  $x$  turns into  $y$  and  $y$  into  $-x$ . The attenuation  $\alpha$ , starting at the point of time  $t=0$ , starting off infinity, is decreasing exponentially. To the present point of time, one can say that there is basically no attenuation anyway. This doesn't apply however considering cosmologic time periods.

At the point of time  $0.897 t_1$  ( $Q=0.947$ ), the function  $\beta$  has a zero-passage. This supplies the somewhat particular course in logarithmic presentation (figure 5). It's about a phase-jump of  $180^\circ$  in this case. From the point of time  $100 t_1$  on we are able to declare, referring to figure 4, the following approximation:

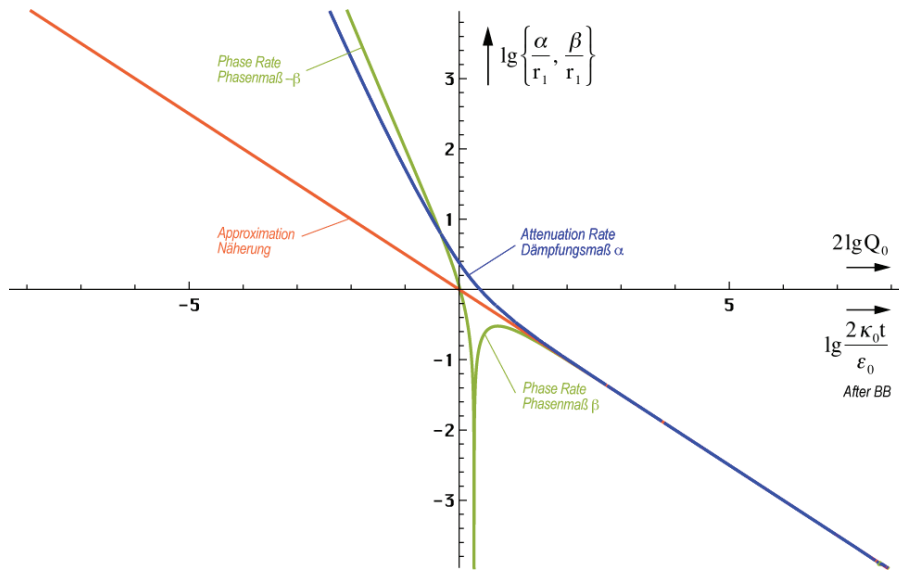


Figure 5  
Phase rate and attenuation rate  
in dependence on time (logarithmic)

$$\underline{\gamma} \approx (1+j)\kappa_0 Z_0 \sqrt[4]{\frac{\epsilon_0}{2\kappa_0 t}} \qquad \underline{\gamma} \approx (1+j) \frac{\kappa_0 Z_0}{\sqrt{2\omega_0 t}} \qquad (39)$$

These relationships can be derived as well graphically from figure 4, as explicitly using (35) by application of (40). However, it's necessary to multiply (35) with  $j$ , in order to take account of the  $90^\circ$  turning (Figure 7). Then, to the approximation  $\underline{\gamma}=2\omega_0/\underline{c}$  is applied. Phase rate and attenuation rate are the same from  $100 t_1$  on approximately. This is the behaviour of an ideal conductor.

For  $\underline{\gamma}$ , we have already found an approximation, still remain  $\underline{c}$  and  $\underline{Z}_F$ . In Figure 3 we have already figured the course of  $\underline{c}$ . To the graphic determination of an approximation, we require the logarithmic representation however (Figure 6). To be considered is the fact, that the imaginary part is actually negative.

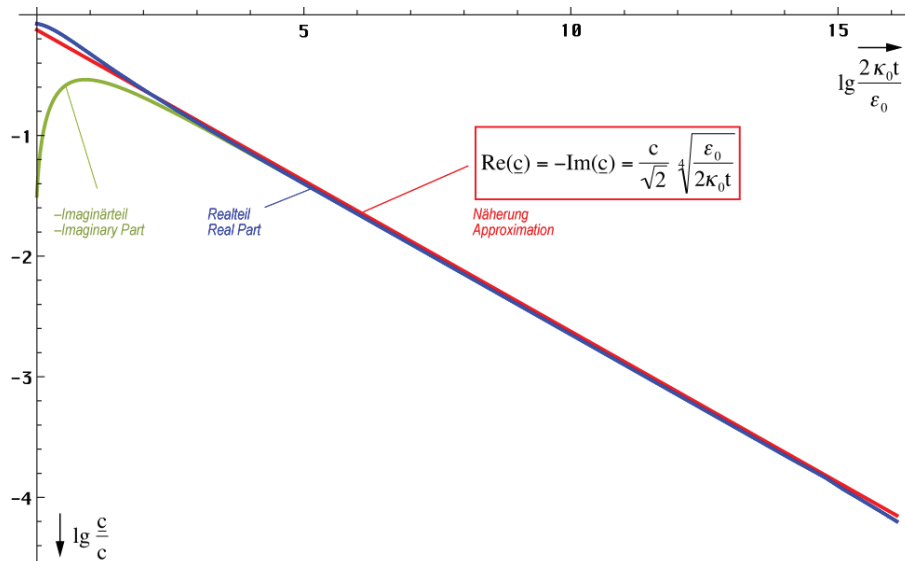


Figure 6  
Propagation-velocity in dependence  
on time (double logarithmic)

$$\underline{c} = \frac{1-j}{\sqrt{2}} c \sqrt[4]{\frac{\epsilon_0}{2\kappa_0 t}} \qquad \underline{c} = \frac{1-j}{2} \frac{c}{\sqrt{\omega_0 t}} \qquad (40)$$

$$|\underline{c}| = c \sqrt[4]{\frac{\epsilon_0}{2\kappa_0 t}} \qquad |\underline{c}| = \frac{c}{\sqrt{2\omega_0 t}} \qquad (1.03807 \cdot 10^{-22} \text{ ms}^{-1}) \qquad (41)$$

$$\underline{Z}_F = \frac{1-j}{\sqrt{2}} Z_0 \sqrt[4]{\frac{\epsilon_0}{2\kappa_0 t}} \qquad \underline{c} = \frac{1-j}{2} \frac{Z_0}{\sqrt{\omega_0 t}} \qquad (42)$$

2.3.2. Expansion curve

At the world-radius, the universe expands with the maximum velocity of 0.851661c, in the inside with a velocity decreasing more and more. Since the wave count in the interior of a sphere with defined radius r(c,t) is decreasing, the deficit is balanced by an increase of wavelength. Outside the wave count ascends continuously due to propagation.

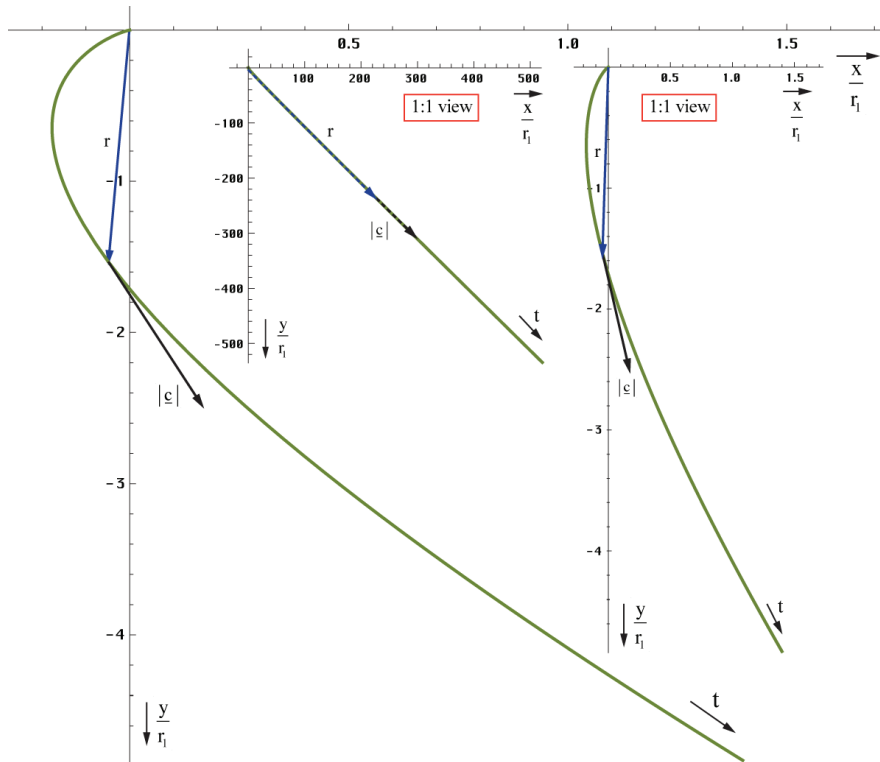


Figure 7  
Track-curve near the singularity  
in dependence on time

For greater t the expansion of the wavefront proceeds nearly rectilinear with an angle of  $-45^\circ$  proportionally  $t^{3/4}$ . But the behaviour looks somewhat different near the singularity. In The track-course of a single sector of wave front near the singularity is shown in figure 7. We see a kind of parabola, with greater t a hyperbola. And there is a rotation in propagation direction about an angle of  $90^\circ$ .

2.3.3. Approximative solution

Now we want to set-up an approximation for the propagation function. The normal form is  $\mathbf{E} = \hat{\mathbf{E}} e^{i\omega t - \gamma x}$  with  $\gamma = \alpha + j\beta$ . But with the exact solution (39) there is a case on hand, with which  $\alpha$  and  $\beta$  contain both damping- and phase-information and the wave function isn't harmonic either. That way we aren't able to form a reasonable propagation function at all.

In the case  $t \gg t_1$  phase- and attenuation rate are of the same size. Thus, the model behaves similar to a metal. There  $\alpha$  does not stand for a damping, but for a rotation, namely as long as, with vertical incidence, a value of  $\pi$  is reached so that the wave exits the metal in the opposite direction after a minimal intrusion. The depth of penetration depends on the material properties, the wave length and the angle of incidence. In case of this model the material properties aren't constant either,  $\gamma$  decreases with  $t$  and  $x$ . Hence it suffices to a rotation of  $90^\circ$  only and the wave remains in the medium (vacuum). In any case, there is a rotation too.

To cope with it, we do a rotation of the coordinate system about  $\pi/4$ . That corresponds to a Multiplikation with  $\sqrt{j}$  and we get a purely imaginary solution. So becomes  $\alpha=0$  and  $\gamma=j\beta$  and the exponentially related attenuation vanishes. Indeed, we still have to multiply the result with  $\sqrt{2}$  and to replace  $x$  by  $r$ . Despite  $\alpha=0$  the amplitudes of  $\mathbf{E}$  and  $\mathbf{H}$  are decreasing continuously. That's caused by the Hankel function alone, resp. by the radical expression in (43).

With it amplitude and phase are firmly interlinked (minimum phase system). Now the rotation angle in space is equal to  $\theta+\pi/4$ . But a separation of phase- and damping-information isn't possible yet. But we can work with very high precision using the approximation equations in this case. To the general Hankel function  $H_0^{(1)}(\omega t - \beta x)$  the following approximation applies (analogously for  $\mathbf{H}$ ):

$$\underline{\mathbf{E}} = \hat{\mathbf{E}} H_0^{(1)}(\omega t - \beta x) \approx \hat{\mathbf{E}} \sqrt{\frac{2}{\pi(\omega t - \beta x)}} e^{j(\omega t - \frac{\pi}{4} - \beta x)} \quad (43)$$

Instead of  $\gamma x$  only the product  $\beta x$  with the phase rate appears in the exponent, since the amplitude rate is already emulated by the radical expression. With  $t \gg 0$  the angle  $\pi/4$  can be omitted. After rotation and transition  $x \rightarrow r$  and  $\omega \rightarrow 2\omega_0$  turns out:

$$\underline{\mathbf{E}} = \hat{\mathbf{E}} H_0^{(1)}(2\omega_0 t - 2\beta_0 r) \approx \frac{2\mathbf{E}_1}{\sqrt{2\omega_0 t - 2\beta_0 r}} e^{j(2\omega_0 t - \frac{\pi}{4} - 2\beta_0 r)} \quad \begin{aligned} H_1 &= \frac{\Phi_1}{\mu_0 r_1^2} \\ E_1 &= \frac{q_1}{\epsilon_0 r_1^2} = \frac{1}{Z_0} \frac{\Phi_1}{\epsilon_0 r_1^2} \end{aligned} \quad (44)$$

$\mathbf{E}_1$  is the peak value of  $\mathbf{E}$  with  $Q_0=1$ . Indeed are both  $\omega=2\omega_0$  and  $\beta=2\beta_0$  (with double frequency even the phase rate must be doubled) no constants at all. That means, they depend on  $t$  and  $r$  at the same time, limiting the manageability of the approximation very much. You can see that also with the phase velocity  $v_{ph}$ . It is defined in the following manner:

$$v_{ph} = \frac{2\omega_0}{\beta} = \frac{2c}{\sqrt{2\omega_0 t}} = 2|c| \quad \text{for } t \gg 0 \quad (45)$$

Thus, the phase velocity is equal to the double absolute value of propagation velocity. That's caused by the factor 2, since phasing with double frequency propagates with double velocity too. For interest, also the group velocity should be stated here:

$$v_{gr} = \frac{1}{d\beta/d\omega_0} = -2|c| \quad \text{for } t \gg 0 \quad (46)$$

Except for the algebraic sign both results are equal. That means, the propagation takes place free from any bias. Further to the approximation. With (22) in section 2.2. we had already found a very good approximation, almost exact, for the same temporal functions

$$\underline{\mathbf{E}} \approx \hat{\mathbf{E}} \sqrt{\frac{2}{\pi}} \frac{e^{j(2\omega_0 t + 2\beta_0 x)}}{\sqrt{2\omega_0 t + 2\beta_0 x}} = 2\mathbf{E}_1 \frac{e^{j(\omega_0 t + \beta_0 r)}}{\sqrt{2\omega_0 t + 2\beta_0 r}} \quad \text{with} \quad \beta_0 = \frac{\kappa_0 Z_0}{\sqrt{2\omega_0 t}} \quad (47)$$

Now, expression (47) enables to define an equivalent- $\alpha=\alpha_0$  and, with it, even an equivalent- $\gamma_0=\alpha_0+j2\beta_0$ , in order to get it up to the normal form for propagation functions.

$$\underline{\mathbf{E}} \approx 2 \mathbf{E}_1 e^{j2\omega_0 t - \gamma_0 r} \quad \text{with} \quad \underline{\gamma}_0 = \frac{1}{2r} \ln \left( 2\omega_0 t + \frac{2\kappa_0 Z_0}{\sqrt{2\omega_0 t}} r \right) + j \frac{2\kappa_0 Z_0}{\sqrt{2\omega_0 t}} \quad (48)$$

That's already a big step forward. Unfortunately, both  $\omega_0$  and  $\gamma_0$  depend on time. It's not critical for  $2\omega_0 t$ , because it's multiplied by  $t$  anyway. Else with  $\gamma_0$ , it should depend on  $r$  only. To the substitution of  $t$  in (49ff) we firstly put (41) left-hand into  $t=r/|c|$ . The real propagation velocity becomes effective here and not  $v_{ph}$  or  $v_{gr}$ . Then we rearrange after  $t$ . Putting into (47) right-hand we get:

$$t = \frac{r}{c} \sqrt[4]{\frac{2\kappa_0 t}{\varepsilon_0}} \quad t^{\#3} = \frac{r^4}{c^4} \frac{2\kappa_0 \cancel{t}}{\varepsilon_0} = 2r^4 \mu_0^2 \varepsilon_0 \kappa_0 \quad (49)$$

$$\beta_0^{12} = \frac{1}{8} \kappa_0^{\cancel{2}8} Z_0^{\cancel{2}8} \frac{\cancel{\varepsilon_0^2}}{\cancel{\kappa_0^2}} \cdot \frac{1}{2r^4 \mu_0^2 \cancel{\varepsilon_0} \cancel{\kappa_0}} = \frac{\kappa_0^8 Z_0^8}{2^4 r^4} \quad \left| \quad \beta_0 = \sqrt[3]{\frac{1}{2r r_1^2}} \quad (50)$$

With it, we obtain for  $\gamma_0$  and the product  $\gamma_0 r$  the following expressions:

$$\underline{\gamma}_0 = \frac{1}{2r} \ln \left( 2\omega_0 t + \left( \frac{2r}{r_1} \right)^{\frac{2}{3}} \right) + j \left( \frac{2}{r r_1^2} \right)^{\frac{1}{3}} \quad \text{for } t \gg 0 \quad (51)$$

$$\underline{\gamma}_0 r = \frac{1}{2} \ln \left( 2\omega_0 t + \left( \frac{2r}{r_1} \right)^{\frac{2}{3}} \right) + j \left( \frac{2r}{r_1} \right)^{\frac{2}{3}} \quad \text{for } t \gg 0 \quad (52)$$

Last but not least the time  $t$  can be completely eliminated. The value  $\gamma_0$  is proportional to  $r^{-1/3}$  and, even more important, the product  $\gamma_0 r$  is proportional to  $r^{2/3}$ . Unfortunately, as already said, we can explicitly state  $\gamma_0(r)$  by approximation only. With the exact function (38) a separation, especially from  $t$  is impossible. But generally speaking, an exact solution is not required at all, since the approximation yields very good results until a striking distance to the particle horizon at  $Q_0=1$ , see figure 2. Therefore, we will not follow up that matter at this point.

All hitherto stated approximations are based on the 4D-expansion-centre  $\{r_1, r_1, r_1, t_1\}$ . But it's more practicable to find a function, related to another centre. Most suitable seems to be the point, where we are, the „point being“. At first we substitute the time according to  $t \rightarrow \tilde{T} + t$ . The swung dash stands for the initial value at the point  $t=0$  (nowadays) describing an inertial system. Hence it's about a constant. Because of  $\tilde{T} = t_1 \tilde{Q}_0^2$  we are able to factor out  $\tilde{Q}_0$ . The direction of time doesn't change. To the temporal part applies:

$$2\omega_0 t = \tilde{Q}_0 \left( 1 + \frac{t}{\tilde{T}} \right)^{\frac{1}{2}} \quad (53)$$

For the spatial part  $\beta_0$  we build up the inertial system once again using the substitution  $r_1 \rightarrow \tilde{R}$ . Because of  $\tilde{R} = r_1 \tilde{Q}_0^2$ , as well as  $\tilde{r} \tilde{Q}_0 = -r$ , now we are measuring from the other end, we can write for  $2\beta_0$ :

$$2\beta_0 = \tilde{Q}_0 \left| \frac{2}{\tilde{r} \tilde{Q}_0 \tilde{r}_1^2 \tilde{Q}_0^2} \right|^{\frac{1}{3}} = -\tilde{Q}_0 \left| \frac{2}{r \tilde{R}^2} \right|^{\frac{1}{3}} \quad \text{Exactly} \rightarrow \quad 2\beta_0 r = -\tilde{Q}_0 \left| \frac{2r - \tilde{r}_0}{\tilde{R}} \right|^{\frac{2}{3}} = -\tilde{Q}_0 \left| \frac{2r}{\tilde{R}} - \frac{1}{\tilde{Q}_0} \right|^{\frac{2}{3}} \quad (54)$$

Actually I should have to write  $\tilde{r}$  instead of  $r$ . But because it's the argument of the function the tilde has been omitted. The right-hand expression considers the fact, that  $r_0$  as smallest increment never can be underrun. The value  $\alpha_0$  is definitely determined by the envelope curve

of the Hankel function, else it would be equal to zero. With it, we obtain for  $\underline{\gamma}_0$  and the product  $\underline{\gamma}_0 r$ :

$$\underline{\gamma}_0 = \frac{1}{2r} \ln \tilde{Q}_0 \left( \left( 1 + \frac{t}{\tilde{T}} \right)^{\frac{1}{2}} - \left( \frac{2r}{\tilde{R}} \right)^{\frac{2}{3}} \right) + j \tilde{Q}_0 \left( \frac{2}{r \tilde{R}^2} \right)^{\frac{1}{3}} \quad (55)$$

$$\underline{\gamma}_0 r = \frac{1}{2} \ln \tilde{Q}_0 \left( \left( 1 + \frac{t}{\tilde{T}} \right)^{\frac{1}{2}} - \left( \frac{2r}{\tilde{R}} \right)^{\frac{2}{3}} \right) + j \tilde{Q}_0 \left( \frac{2r}{\tilde{R}} \right)^{\frac{2}{3}} \quad (56)$$

With  $r_0$  we have already found one elementary length. But LANCZOS speaks about another one [1]. That's the wave length of the metric wave field  $\lambda_0 = 2\pi/\beta$ . The approximation of  $\lambda_0$  must be divided by 2 once again, due to the double phase velocity. Hence  $\lambda_0 = 2\pi/\beta_0$  applies. To the comparison the expression for  $r_0$  once again:

$$\lambda_0 = \frac{2\pi}{\rho_0(2\omega_0 t) \kappa_0 Z_0} \operatorname{cosec} \frac{1}{2} \arctan \theta(2\omega_0 t) \quad (57)$$

$$\lambda_0 = \frac{\pi}{\kappa_0 Z_0} \sqrt[4]{\frac{2\kappa_0 t}{\varepsilon_0}} = \frac{\pi}{\kappa_0 Z_0} \sqrt{2\omega_0 t} \quad \text{for } \omega_0 t \gg 0 \quad (58)$$

$$r_0 = \frac{1}{\kappa_0 Z_0} \sqrt[4]{\frac{2\kappa_0 t}{\varepsilon_0}} = \frac{2\omega_0 t}{\kappa_0 Z_0} = \sqrt{\frac{2t}{\kappa_0 \mu_0}} \quad (59)$$

Though  $\lambda_0$  is smaller than  $r_0$  and not identical to HEISENBERG's elementary length with it.  $\lambda_0$  now is in the range of  $10^{-68}$  m. Thus, LANCZOS was wrong in that point. But it only has been a guess on his part. In fact, it's about the wave length of the wave function forming the metric lattice itself. Expression (57) until (59) only represent the temporal functions. Then, the functions of time and space read as follows.

$$\lambda_0 = \frac{2\pi}{\rho_0(2\omega_0 t - \underline{\gamma}_0 r) \kappa_0 Z_0} \operatorname{cosec} \frac{1}{2} \arctan \theta(2\omega_0 t - \underline{\gamma}_0 r) \quad (60)$$

$$\lambda_0 = \pi r_0 \tilde{Q}_0^{-\frac{1}{2}} \left( \left( 1 + \frac{t}{\tilde{T}} \right)^{\frac{1}{2}} - \left( \frac{2r}{\tilde{R}} \right)^{\frac{2}{3}} \right)^{\frac{1}{2}} = \frac{\pi}{\kappa_0 Z_0} \sqrt{2\omega_0 t - 2\beta_0 r} \quad (61)$$

$$r_0 = dr = \tilde{r}_0 \left( \left( 1 + \frac{t}{\tilde{T}} \right)^{\frac{1}{2}} - \left( \frac{2r}{\tilde{R}} \right)^{\frac{2}{3}} \right) = \frac{2\omega_0 t - 2\beta_0 r}{\kappa_0 Z_0} \quad (62)$$

The wave length  $\lambda_0$  of the metrics is irrelevant for the further contemplations of this work, only  $\beta_0$  matters. The double-bracketed expression in (62) is called *Navigational Gradient* in future. It is the essential expression I was looking for.

We only know the local age  $T$ , which results from the local HUBBLE-parameter (249). It quasi represents the temporal distance to the expansion centre. But we are able to determine the spatial distance to the world radius  $R$ . This forms a spatial singularity (event horizon) with it. The value arises from the ansatz (250):

$$2\omega_0 t - \beta_0 r = \frac{\omega_0(H)}{H} \quad \text{with } r = 0 \quad T = \frac{1}{2H} \quad (63)$$

$$R = -\frac{\omega_0(H)}{\beta_0 H} = -\frac{\omega_0 r_0}{H} = -2ct \quad \text{with } 2\omega_0 t = 0 \quad (64)$$

$$\beta_0 = \kappa_0 Z_0 \sqrt[4]{\frac{\varepsilon_0 H}{\kappa_0}} = \sqrt{\frac{c^3}{G\hbar}} = \frac{1}{r_0} \quad (65)$$



Hence, the value of  $\beta_0=1/r_0$  even can be obtained from (39), in that we replace time with the HUBBLE-parameter  $H_0$ . To R applies:

$$R = -\frac{c}{H_0} = -1.22471 \cdot 10^{26} \text{ m} = -1.2946 \cdot 10^{10} \text{ Ly} = -3.96896 \text{ Gpc} \quad (66)$$

$$R = -\frac{c}{H_0} = -1.34803 \cdot 10^{26} \text{ m} = -1.4249 \cdot 10^{10} \text{ Ly} = -4.36862 \text{ Gpc} \quad (67)$$

That's about 13 billion light years for  $H_0=71.9963 \text{ kms}^{-1} \text{ Mpc}^{-1}$ . The result (67) for the alternative value of  $H_0=68.6241 \text{ kms}^{-1} \text{ Mpc}^{-1}$  has been calculated with the help of ([9] 1049) and the CODATA<sub>2018</sub>-values. The local age has the character of a time-constant and amounts only to the half, namely 6.6/7.1 billion years. The world radius (great circle) is equal to  $cT$ . More extended time-like vectors up to  $2cT$  are possible due to expansion and propagation of the metric wave field. Full particulars in the next sections.

The wave field examined here, forms the metrics of the universe (empty space), the real (nearly) MINKOVSKIAN line element. We can already declare it here. Further contemplations are done in section 7.2.1. of [10]. We act on ([10] 0.23) in it's differential form in that we replace the otherwise usual light speed  $c$  with the propagation velocity  $\underline{c}$  of the metric wave field:

$$ds^2 = dx^2 + dy^2 + dz^2 - \underline{c}^2 dt^2 \quad \text{or} \quad (68)$$

$$ds^2 = dr^2 + r^2(d\vartheta^2 + \sin^2\vartheta d\varphi^2) - \underline{c}^2 dt^2 \quad (69)$$

Here immediately becomes clear, which physical meaning is assigned to the MLE. For the exact formula, we usefully apply polar-coordinates.. We now substitute the exact expression for  $\underline{c}$  ( $r=0$ ) obtaining:

$$ds^2 = dr^2 + r^2(d\vartheta^2 + \sin^2\vartheta d\varphi^2) - \frac{c^2 dt^2}{4\omega_0^2 t^2 \rho_0^2 (2\omega_0 t - \underline{\gamma}r)} (\sin \frac{1}{2} \arctan \theta (2\omega_0 t - \underline{\gamma}r) - j \cos \dots)^2 \quad (70)$$

$$ds^2 = dr^2 + r^2(d\vartheta^2 + \sin^2\vartheta d\varphi^2) + \frac{c^2 dt^2}{4\omega_0^2 t^2 \rho_0^2 (2\omega_0 t - \underline{\gamma}r)} (\cos \arctan \theta (2\omega_0 t - \underline{\gamma}r) + j \sin \dots) \quad (71)$$

$$ds^2 = dr^2 + r^2(d\vartheta^2 + \sin^2\vartheta d\varphi^2) + \frac{c^2 dt^2}{4\omega_0^2 t^2 \rho_0^2 (2\omega_0 t - \underline{\gamma}r)} \frac{1 + j\theta(2\omega_0 t - \underline{\gamma}r)}{\sqrt{1 + j\theta^2(2\omega_0 t - \underline{\gamma}r)}} \quad (72)$$

$$ds^2 = dr^2 + r^2(d\vartheta^2 + \sin^2\vartheta d\varphi^2) + \frac{c^2 dt^2}{4\omega_0^2 t^2 (1 - A^2(\phi) + B^2(\phi))(1 - j\theta(\phi))} \quad (73)$$

$$ds^2 = dr^2 + r^2(d\vartheta^2 + \sin^2\vartheta d\varphi^2) + \frac{dr_0^2}{1 - (A(\phi) - jB(\phi))^2} \quad \text{because of} \quad \dot{r}_0 dt = dr_0 \quad (74)$$

with  $\phi = 2\omega_0 t - \underline{\gamma}r$ . Interesting is the algebraic sign-reversal. The cone turns into a ball. The previous light cone however continues to be applied to overlaid signals always propagating with  $c$ . It adds up the local propagation-velocity (not expansion-velocity!).  $A(\phi)$  and  $B(\phi)$  determine the rotation near the singularity. The reciprocal of the expression in the denominator shows a behaviour like  $t^{1/2}$ . Now still the approximation:

$$ds^2 \approx dr^2 + r^2(d\theta^2 + \sin^2\theta d\varphi^2) + (\phi - \frac{1}{2}) dr_0^2 \quad (75)$$

$$ds^2 \approx dr^2 + r^2(d\theta^2 + \sin^2\theta d\varphi^2) + Q_0 dr_0^2 \quad (76)$$

$$ds^2 = dr^2 + r^2(d\vartheta^2 + \sin^2\vartheta d\varphi^2) + \tilde{c}^2 \left( \left( 1 + \frac{t}{\tilde{T}} \right)^{\frac{1}{2}} - \left( \frac{2r}{\tilde{R}} \right)^{\frac{2}{3}} \right)^{-1} \quad (77)$$



### 3. Expansion, topology and entropy

In section 2.3.3. we found with (62) an expression for the temporal and spatial dependence of PLANCK's elementary-length  $r_0$ , figuring at least locally a scale for the proportions (distance). On this occasion I refer once again to the fact that this is *also* applied to the size of material bodies, which is changing in the same measure as  $r_0$ . Otherwise we could not observe any expansion either.

Just particularly is this a matter of the mutual distances of material bodies. These follow a function, which differ with the considered distance, since quantity and expansion-velocity of the PLANCK elementary-length is changing with ascending distance to the coordinate-origin. But only distances with their starting-point in the origin should will be considered here. Of considerable importance for deeper contemplations is even the number of line elements (MLEs) along an imagined line with the length  $r$  (wave count vector  $\Lambda$ ).

We distinguish two cases in this connection: Wave count vector with constant  $r$  and  $r$  with constant wave count vector. More final case to the best fits the existing circumstances, since we can assume that no point is distinguished to other points in the cosmos. The average relative velocity against the metrics at the coordinate-origin is equal to zero at free fall. This should be so everywhere then. With it, the expansion of the universe can be traced back to the expansion of the metrics alone. This corresponds to the case of a constant wave count vector.

#### 3.1. Expansion

##### 3.1.1. Constant distance

Because of the *real lattice constant*  $r_0$  the wave count vector  $\Lambda$  for smaller distances  $r$  is defined in the following manner:

$$\Lambda = \frac{r}{r_0} \mathbf{e}_r \quad (78)$$

$\mathbf{e}_r$  is the unit-vector. In the following, we consider only the figure  $\Lambda$  however. For larger distances, we have to replace  $\Lambda$  by  $d\Lambda$  and  $r$  by  $dr$  using the corresponding expression (62) for  $r_0$ :

$$d\Lambda = \frac{1}{\tilde{r}_0} \frac{dr}{(1+t')^{\frac{1}{2}} - \left(\frac{2r}{\tilde{R}}\right)^{\frac{2}{3}}} \quad \text{with } t' = \frac{t}{\tilde{T}} \quad (79)$$

To the solution we replace as follows (it applies  $\tilde{R}/\tilde{r}_0 = \tilde{Q}_0$ ):

$$d\Lambda = \frac{3}{2} \frac{\tilde{R}}{\tilde{r}_0} \frac{r'^2}{a^2 - r'^2} dr' \quad \text{mit } r' = \left(\frac{2r}{\tilde{R}}\right)^{\frac{1}{3}} \quad \left| \quad a^2 = (1+t')^{\frac{1}{2}} \quad \right| \quad dr = \frac{3}{2} \tilde{R} r'^2 dr' \quad (80)$$

$$\Lambda = \frac{3}{2} \tilde{Q}_0 \int \frac{r'^2}{a^2 - r'^2} dr' = \frac{3}{2} \tilde{Q}_0 \left( a \operatorname{artanh}^*) \frac{r'}{a} - r' \right) \quad \begin{array}{l} *) \operatorname{arcoth} \text{ for } |r'| > a \\ \text{(behind the particle horizon)} \end{array} \quad (81)$$

$$\Lambda = \frac{3}{2} \tilde{Q}_0 \left( \left(1 + \frac{t}{\tilde{T}}\right)^{\frac{1}{4}} \operatorname{artanh} \left( \frac{\left(\frac{2r}{\tilde{R}}\right)^{\frac{1}{3}}}{\left(1 + \frac{t}{\tilde{T}}\right)^{\frac{1}{4}}} - \left(\frac{2r}{\tilde{R}}\right)^{\frac{1}{3}} \right) \right) \quad \text{def } \Lambda_0 = \frac{R}{2r_0} = \frac{Q_0}{2} \quad (82)$$

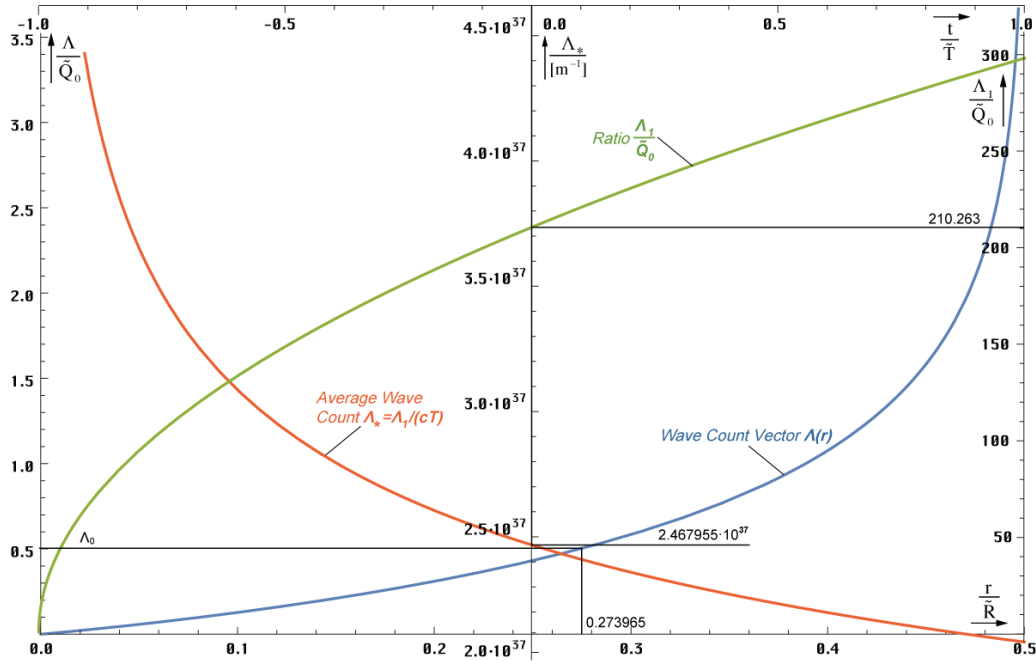


Figure 8  
Wave count vector as function  
of distance r and t

The wave count  $\Lambda$  follows the blue function depicted in figure 8. Approaching to half the world radius ( $R/2$ ), it seems to be, that  $\Lambda$  strives towards infinity. If we want to define a finite wave count  $\Lambda_0$ , we take only a certain part of the world radius to calculate the wave count for it. Because of  $R/(2r_0) = Q_0/2$  we opt for that value. The value amounts to  $0.273965R$ , that is 54.79% of the distance to the particle horizon ( $cT$ ). In total however an infinite value will not be reached, since  $r_0$  becomes smaller and smaller going to  $r_1$ . Out there, at  $Q=1$  is the back of beyond, we reached the particle horizon.

At first I guessed the value to be  $\Lambda_1 = Q_0^2$ , since even  $R = r_1 Q_0^2$  applies. But that's not the case. The little more ambitious calculation for  $r = R/2 - r_1 \rightarrow 1 - 10^{-120}$  under application of the power series for  $(1-x)^{1/3}$ , multiple substitutions up to the transformation of the function  $\text{artanh} \rightarrow \text{arsinh} \rightarrow \ln$ , turns out  $\Lambda_1 = \frac{3}{2} Q_0 \ln Q_0 \approx 210 Q_0 = 1.75495 \cdot 10^{63}$  using the values from table 1. For  $\Lambda_1$  applies  $t' \equiv t \equiv 0$  i.e. a constant wave count vector. But by expansion and wave propagation »outwards« the phase angle  $2\omega_0 T = Q_0 \sim t^{1/2}$  increases continuously. And because of (4)  $\Lambda_1(T) = \frac{3}{2} \sqrt{bT} \ln \sqrt{bT}$  applies with  $b = 2\kappa_0/\epsilon_0$ .

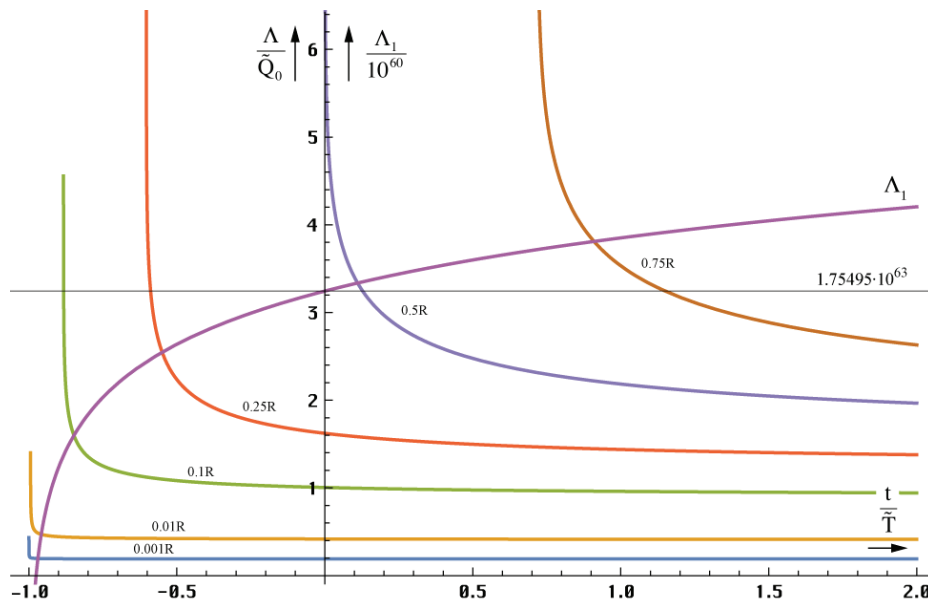


Figure 9  
Temporal dependence of the wave count vector  
for several distances r

The temporal dependence for several initial distances  $r$  is shown in figure 9. The larger the considered length, the later on the point of time, the wave count vector is defined from. That's easy to understand, we can regard a length as existent only then, when the world-radius is larger or equal to. If the world-radius is smaller, so such a length doesn't exist. Therefore, lengths larger than  $0.5R$  aren't defined at present and function (82) does not have a real solution before a value of e.g.  $t=0.75T$  is reached ( $t=0$  is the present point of time). Altogether, the wave count decreases. That results from the fact that we are considering a constant length with expanding  $r_0$ . So it happens, that MLEs are permanently „scrolled out“ at the „tail“ leading to a degradation of the wave count vector at the same time.

### 3.1.2. Constant wave count vector

#### 3.1.2.1. Solution

At first we start with the left expression of (82) for  $t=0$  ( $a=1$ ). It specifies the quantity of the wave count vector at the present point and at each point of time, if we want to assume it as constant. We just look for the function  $F(a, \tilde{r}')$  being nothing other as the temporal dependence on a given length  $\tilde{r}'$ . See (80) for  $a(t)$ .

$$\Lambda = \frac{3}{2} \tilde{Q}_0 \operatorname{artanh} \tilde{r}' - \tilde{r}' = \frac{3}{2} \tilde{Q}_0 \left( a \operatorname{artanh} \frac{\tilde{r}' F}{a} - \tilde{r}' F \right) = \text{const} \quad (83)$$

An explicit reduction by differentiating and zero-setting (the left expression turns to zero on this occasion) leads to the trivial solution  $F=0$ . Otherwise, only an implicit solution can be found as solution of the equation:

$$a \operatorname{artanh} \frac{\tilde{r}' F}{a} - \operatorname{artanh} \tilde{r}' - \tilde{r}' (F - 1) = 0 \quad r(t) = \tilde{r}' F^3(t) \quad (84)$$

or in »Mathematica«-notation  $F1[t,r]$ :

$$\begin{aligned} \text{Fa1} &= \text{Function}[a = \text{FindRoot}[\#1 * \text{ArcTanh}[\#2 / \#1 * \kappa] - \text{ArcTanh}[\#2] - \\ &\#2 * (\kappa - 1) == 0, \{\kappa, 1\}, \text{MaxIterations} \rightarrow 30]; (\text{Round}[(\kappa / .a) * 10^7 / 10^7]^3); \\ \text{F1} &= \text{Function}[\text{Fa1}[(1 + \#1)^\wedge{.25}, (2 * \#2)^\wedge{(1/3)}]]; \end{aligned} \quad (85)$$

In this connection we have to be particular about the method (tangent-method) and the initial value. There was a problem using secant method. The temporal course is shown in figure 10.

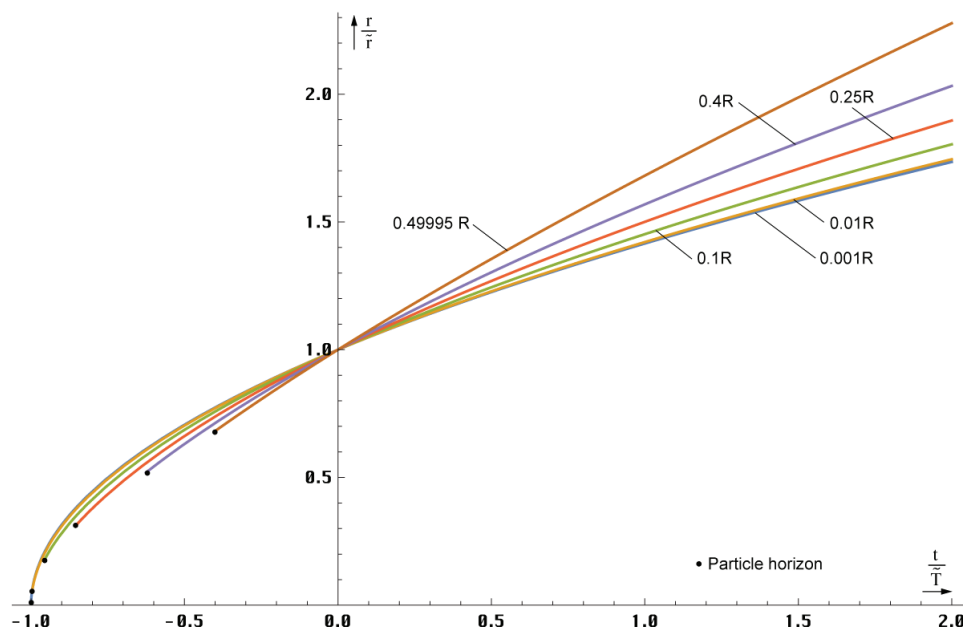


Figure 10  
Temporal dependence  
of a given distance  $r$

There is only a limited definition-range for the solution. It is temporally bounded below by the spatial singularity, the considered length is greater than the world-radius and doesn't exist yet. The greater the considered length, the smaller the definition range. With world-radius the space-like vector  $R/2 = cT$  is meant.

### 3.1.2.2. Approximative solutions

A simple solution for small  $r$  explicitly arises from (84) under application of the two first terms of the TAYLOR series for the function  $\text{artanh}$ :

$$r = \tilde{r} \left(1 + \frac{t}{\tilde{T}}\right)^{\frac{1}{2}} \approx \tilde{r} \left(1 + \frac{1}{2} \frac{t}{\tilde{T}}\right) \quad \text{for } \tilde{r} \leq 0.01 \tilde{R} \quad (86)$$

This exactly corresponds to the behaviour of PLANCK's elementary-length (MLE) and is valid until  $0.01R$  approximately. For larger distances, the ascend is larger. First we examine the course in the proximity of  $t=0$  (figure 11) as well as the ascend  $\Delta r/\Delta t$  with  $\Delta t = 2 \cdot 10^{-3}$ . With root-functions the ascend ( $dr/dt$ ) is equal to the exponent  $m$  in this point:

$$r = \tilde{r} \left(1 + \frac{t}{\tilde{T}}\right)^m \approx \tilde{r} \left(1 + m \frac{t}{\tilde{T}}\right) \quad (87)$$

This is shown in figure 11. It is in the range of  $1/2 \dots 3/4$ . Using the function  $\text{Fit}[]$  with the help of (88) approximations of different precision for the exponent  $m$  can be found:

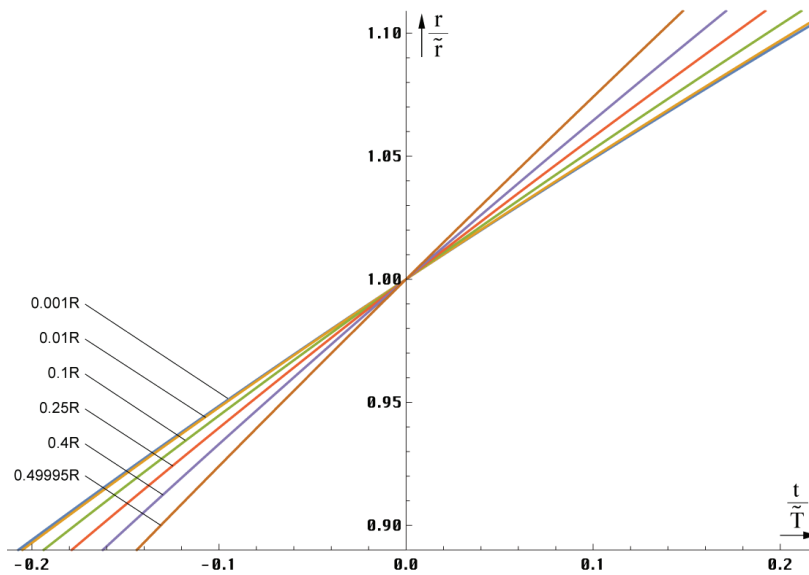


Figure 11  
Ascend of several  
given distances in  
the proximity of  $t=0$

```
mmm = {{0, .5}};
For[x = 0; i = 0, x < .499, (++i), x += 0.01;
AppendTo[mmm, {x, N[F1[0.0001, x] - F1[0, x]]/0.0001}]]
Fit[mmm, {1, m, m^2, m^3, ...}, m] (88)
```

$$m \approx 0.513536 + 0.17937r + 0.490927r^2 \quad \text{with } r = r/\tilde{R}$$

$$m \approx 0.500(980) + 0.50052r - 1.13082r^2 + 2.16233r^3 \quad (89)$$

$$m \approx 0.500(1002) + 0.598206r - 3.45991r^2 + 18.3227r^3 - 42.6995r^4 + 38.0733r^5$$

The third equation of (89) is very exact and suitable even for calculations with more extreme demands. Indeed, there is a need to consider the restricted definition-range, which is not

being co emulated automatically by the approximative solution. It is pointed out here once again that the distances and velocities, regarded in this section, are a matter of space-like vectors having nothing to do with the time-like vectors considered in section 4.3.4.4.6. of [1] Cosmologic red-shift.

### 3.1.2.3. The HUBBLE-parameter

Having defined the HUBBLE-parameter only for small lengths and PLANCK's elementary-length ( $r_0$ ) until now, which are following the relationships for a radiation-cosmos ( $m=1/2$ ), we have to correct our statements for larger distances. With  $m=m(r)$  the HUBBLE-parameter  $H=r/\dot{r}$  becomes also a function of distance:

$$H = \frac{m}{\tilde{T} + t} \qquad H_0 = \frac{m}{\tilde{T}} \qquad (90)$$

The course is shown in figure 12. The metrics examined by this model is a non-linear metrics. With it, the question has become unnecessary, whether our universe is a radiation- or dust-cosmos. The answer is – as well, as. It's a question of the dimensions of the considered area. For small lengths, the distance behaves like a radiation-cosmos, in the range between zero and  $0.5R$  like a dust-cosmos, with  $0.5R$  like photons overlaid the metrics.

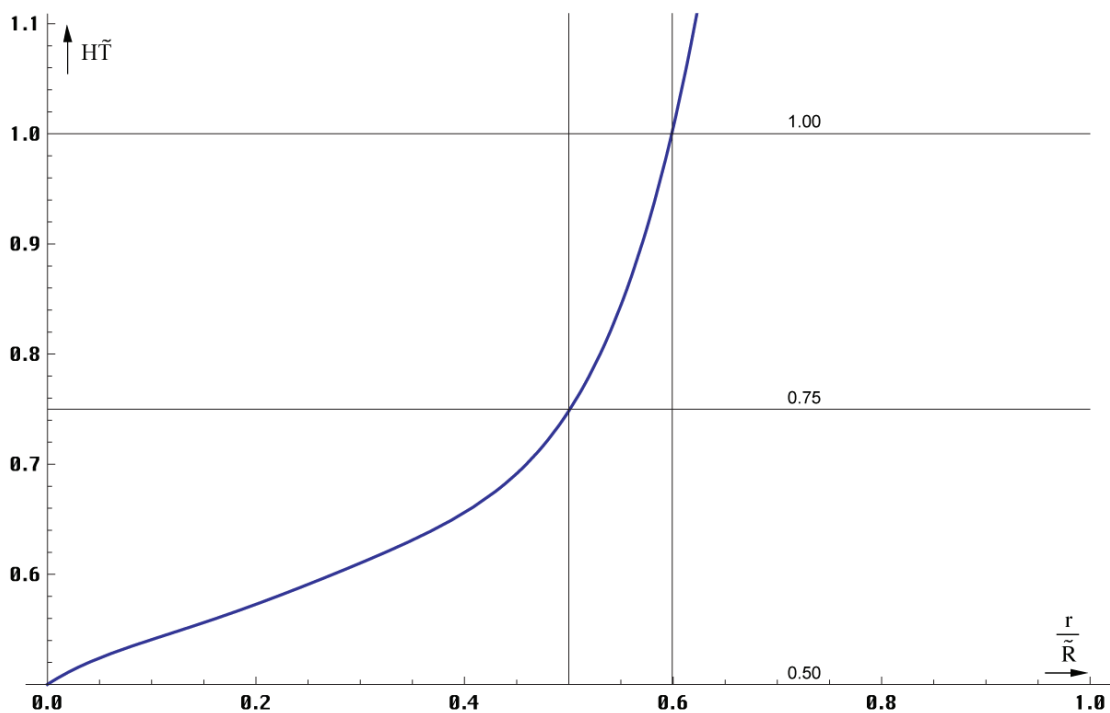


Figure 12  
HUBBLE-parameter as a function of the distance for  $t=0$ , the values  $r>0.5R$  are extrapolated.

However, more latter distance is not an area of infinite red-shift as in other models. It shows with the dilatory-factor  $q$  very well The course is depicted in figure 13.

$$q = -\frac{r\ddot{r}}{\dot{r}^2} = \frac{1}{m} - 1 \qquad (91)$$

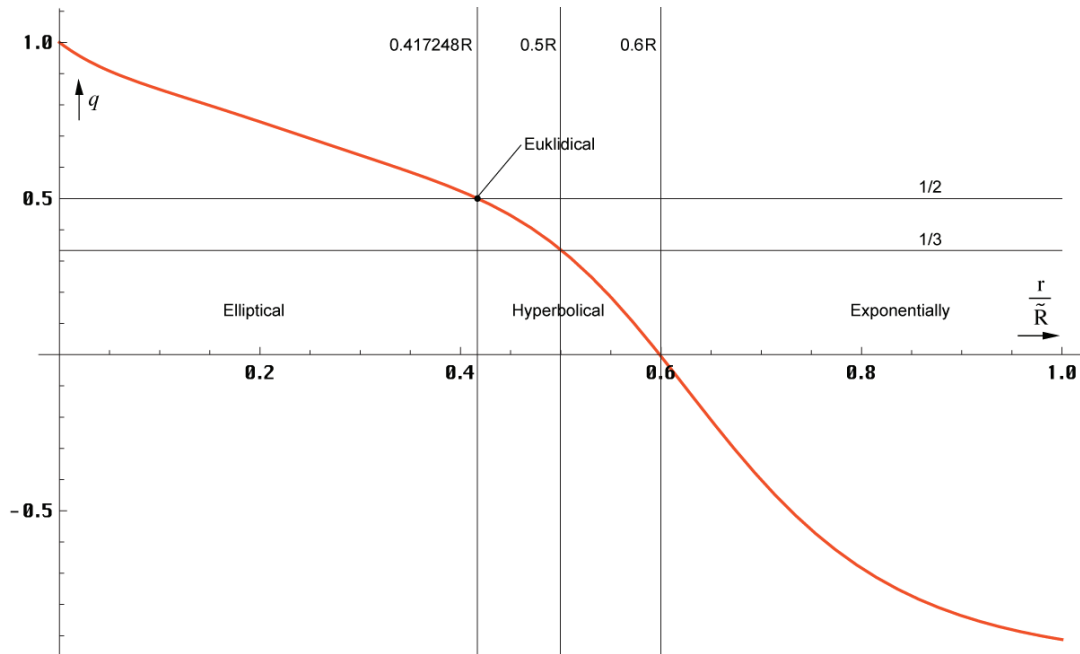


Figure 13  
Dilatory-factor as a function of the distance for  $t=0$ , the values  $r > 0.5R$  are extrapolated

The expansion-velocity  $H_0r$  as a function of the distance is shown in figure 14. The speed of light is reached in an essentially minor distance as with the standard-models, but only on paper. While the size of  $r_0$  at  $0.5R = cT$  tends to  $r_1$ , the expansion speed along the time-like world line at this point is not infinite, rather it's smaller than  $c$  ( $0.75c$ ).

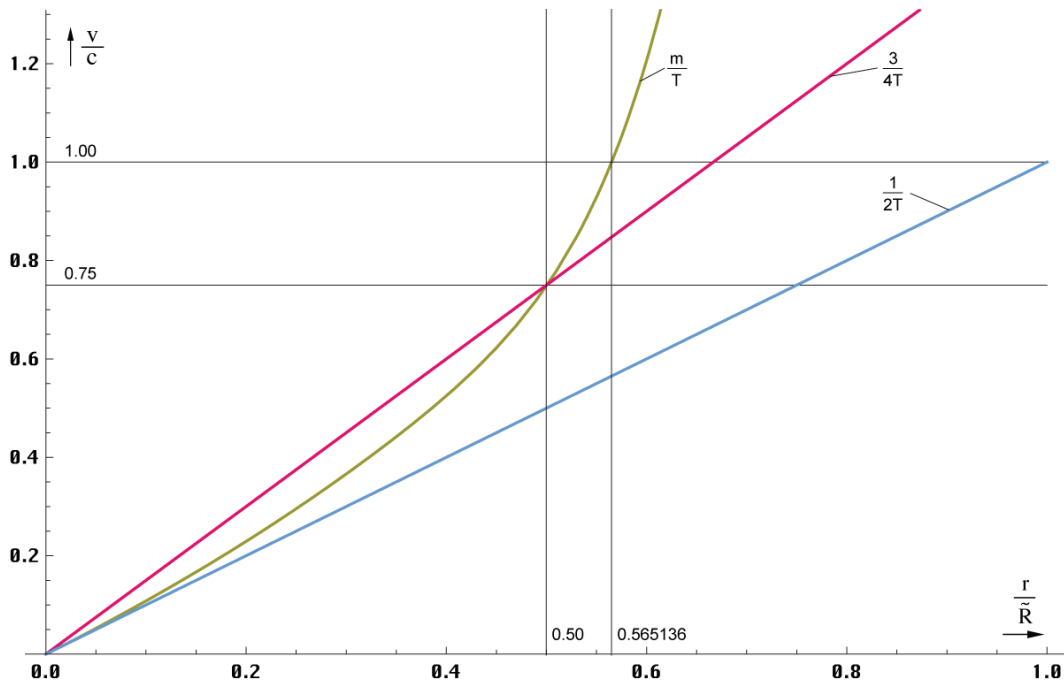
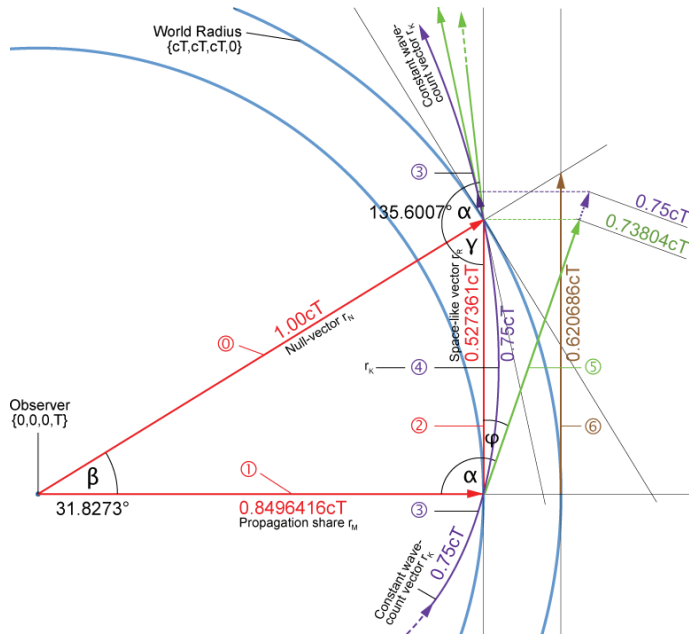


Figure 14  
Expansion-velocity as a function of the distance for  $t=0$ , the values  $r > 0.5R$  are extrapolated

Otherwise we found out, that the maximum propagation speed  $|c_{\max}|$  of the metric wave field amounts to  $0.851661c$  only. But furthermore the world-radius should be  $cT$ , whereas time-like vectors with up to  $2cT$  should be possible.



So we have to do with four different distances resp. velocities, which all does not seem to fit together anyhow. But using this model it's possible to solve this conflict. Let's have a look on Figure 15, which except for  $r_K$ , is a true-to-scale representation.

We assume, that the wave front of the metric wave field propagates straight-forward with  $0.851661c$ . It corresponds to the vector ① in Figure 15 thus to the propagation share.

Figure 15  
Expansion-velocity and world-radius in the model

Then, the share  $r_M$  of the world-radius caused by it would amount to  $0.851661cT$ . However, other values are given in the figure, why, we will see later. As noticed furthermore, the constant wave count vector  $r_K$  up to the vicinity of  $R/2$  is running on the same track as the incoming time-like vector  $r_T$  with  $0.75c$  (arc length  $0.75cT$ ). But it's tilted about the angle  $\alpha_1$ , so that we have to sum geometrically. In addition the partial vector ④ is curved. But the object we are looking for is the space-like vector  $r_R$  (expansion share ②). Next we flatten the partial vector ④ bending it up to ⑤. Then we project it onto  $r_R$ , it applies  $r_R = -r_K \cos\varphi$  with the angle  $\varphi = \arg \underline{c} = \alpha - \pi/2 = 48.6231^\circ$  of the metric wave function. With a phase angle of  $Q = 0.8652911138$  we obtain with the angle  $\alpha = 2.419430697 \pm 138.6231678^\circ$  the following solution:

$$c = \sqrt{c_M^2 + c_R^2} = \sqrt{c_M^2 + c_K^2 \cos^2 \alpha} = c\sqrt{0.85166^2 + 0.75^2 \cos^2 2.41943} \quad (92)$$

$$c = c\sqrt{0.85166^2 + 0.562784^2} = 1.02081c \quad \Delta = +2.08 \cdot 10^{-2} \quad (93)$$

This result isn't notably exact since values for  $\beta$ ,  $\varphi$  and  $c_M$  have been used, misfitting  $Q = 1$ . We will see, if we are able to get a more exact result. If we get granular on Figure 15, we see, that  $r_K$  is curved and, even in this state, protrudes significantly beyond  $r_R$ . As the case may be, we have to impose it with a correction factor, if we want to get a correct relation. On the one hand there is the ratio  $RS = r_K/r_N$ , which we can calculate. On the other hand there will be a similar case with the classic electron radius in section 3.3.2.3. of [10], where we defined a correction factor  $\zeta = 1.01619033$ . Since I wonder about it exactly, I calculated a great many of alternatives, but neither the correction factor  $\zeta$  nor  $RS = r_K/r_N$  proved to be particularly helpful.

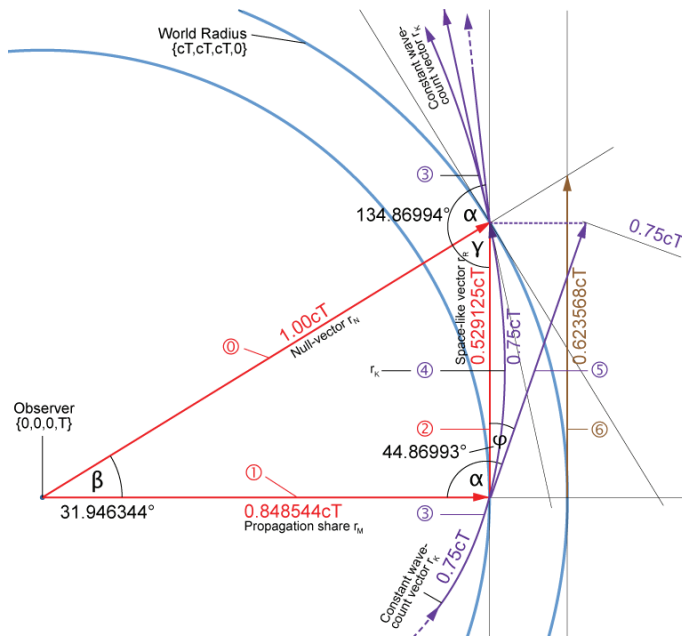
But there is a version, which delivers an acceptable result even without a correction factor. That's *the* case, with which the real part of the wave function  $\underline{c}_M$  (27) has a zero-crossing (phase-jump). Since it's the simplest variant, it's probably the right one and I will prioritize it. See [10] for details. Here the exact parameters for this variant:

$$\begin{array}{llll} Q = 0.95013820167858442645 & c_M = 0.8485439825230016c & c_R = 0.529124852680352c & c_K = 0.75c \\ \alpha = 134.86993657768931460^\circ & \beta = 31.94634370109298^\circ & \varphi = 44.8699365776893146^\circ & RS = 1.02469672804290424 \end{array}$$

$$c = \sqrt{c_M^2 + c_K^2 \cos^2 \alpha} = c\sqrt{0.848544^2 + 0.529125^2} = 1.0000000c \quad \Delta = \pm 0.000000 \quad (94)$$

The conclusion is, the universe expands behind the particle horizon at  $Q = 0.9501382$ . That's between the point with the maximum expansion velocity and  $Q = 1$ . It is reminiscent of a surfer, who does not run on the crest of waves, but always a little off. With it, we have clarified the contradictions between the various world radii and expansion velocities. According





to the name, it's a kind of LEHU (Light speed Expanding Hyperspherical Universe) similar to [11] but without Standard Model and with totally different basics.

Please find more information about the time-like vector  $r_T$  in section 5. The knowledge gained here has a significant influence on the calculation of the entropy of the metric wave field.

Figure 16  
Expansion-velocity and world-radius without correction factor

### 3.2. Energy and Entropy

#### 3.2.1. Entropy

Now we will consider the discrete MLE and our model from the energetic point of view. Since entropy is much more important than energy for the thermodynamician, we will take it into account by examining entropy first. We want to mark entropy with  $S$  henceforth. In order to avoid confusions with the POYNTING-vector, we will always figure it bold as vector ( $\mathbf{S}$ ). If we write  $S$ , we always mean entropy and with  $\mathbf{S}$  always the POYNTING-vector.

From the statistic point of view, the entropy of a system is defined by (95) where  $k$  is the BOLTZMANN-constant and  $N$  the number of all possible inner configurations.

$$S = k \ln N \tag{95}$$

With a single MLE ( $N=1$ ) entropy would be equal to zero theoretically. That's wrong of course, since statistics necessitates a minimum number of  $N$  to be applied at all. With  $N=1$  the result, mathematically can take on a whatever value without offending the »statistics«. Therefore we want to try to find out, if there is another possibility to determine the entropy of this single MLE.

Strictly speaking the MLE is a matter of a ball-capacitor with the mass  $m_0$  moving in its inherent magnetic field. We don't know what happens inside the capacitor. Basically it behaves like a (primordial) black hole. According to [7] the SCHWARZSCHILD-radius of such a BH is defined as:

$$r_s = \frac{2mG}{c^2} \tag{96}$$

Now let's substitute  $m$  with  $m_0$  here (2). We get  $r_s=2r_0$ , substantiating our foregoing assumption. The surface of this black hole yields with it to  $A=4\pi r_0^2$ . It's interesting that the expression for the SCHWARZSCHILD-radius can be derived even without aid of the SRT or URT. Because both, SRT and URT according to this model are only emulated by the metric fundamental lattice. Such relationships must be basic qualities of the lattice itself. They apply as well microscopically as macroscopically then.



In [8] pp. 211 a method is figured to determine the entropy of a black hole. It is based on quantum physical considerations fitting our MLE very well. The author assumes the KERR-NEWMAN-solution of the EINSTEIN-vacuum-equations  $R_{ik}=0$  with stationary rotating, electrically loaded source and external electromagnetic field (97) with  $R \equiv r^2 - 2mr + a^2$  and  $\rho^2 \equiv r^2 + a^2 \cos^2 \vartheta$ ,  $M = mGc^{-2}$  und  $a = Lm^{-1}c^{-1}$ ;  $m$  is the mass and  $L$  the moment of momentum.

$$ds^2 = -\frac{R}{\rho^2} [c dt - a \sin^2 \vartheta d\varphi]^2 + \frac{\rho^2}{R} dr^2 + \rho^2 d\vartheta^2 + \frac{\sin^2 \vartheta}{\rho^2} [(r^2 + a^2) d\varphi - a dt]^2 \quad (97)$$

We don't want to engross it here. The author finally comes to the following statements for the radius  $r_{\pm}$  of the black hole and its surface  $A$ :

$$r_{\pm} = M \pm \sqrt{M^2 - a^2} \quad A = 8\pi \left[ M^2 \pm M\sqrt{M^2 - a^2} \right] \quad (98)$$

$$r_{\pm} = \sqrt{\frac{2t}{\mu_0 \kappa_0}} \pm \sqrt{\frac{2t}{\mu_0 \kappa_0} - \left( \frac{2t}{\mu_0 \kappa_0} \right)_{L=\hbar}} \quad r_{\pm} = r_0 \pm \sqrt{r_0^2 - (r_0^2)_{L=\hbar}} \quad (99)$$

The result depends thereon, if the MLE disposes of a moment of momentum or not. With  $m=m_0$  under application of (2), (4) and (868 [10]) we obtain the following values for the SCHWARZSCHILD-radius: Without moment of momentum ( $L=0$ ) for  $r_-=0$ ,  $r_+=r_s=2r_0$  as well as  $A=4\pi r_0^2$ . With moment of momentum  $L=\hbar$ , here the brackets apply, we get two identical solutions  $r_{\pm}=r_0$ . The surface yields  $A=\pi r_0^2$ .

Furthermore, the author refers to a work of BEKENSTEIN (1973), according to which the entropy of a black hole should be proportionally to its surface. The exact proportionality-factor has been determined by HAWKING (1974) in a quantum physical manner to:

$$S_b = \frac{kc^3}{4G\hbar} A = k \frac{A}{4r_0^2} = k \frac{A}{(4)r_s^2} \quad (100)$$

$k$  is the BOLTZMANN-constant, the bracketed number applies to  $L=\hbar$ . Interestingly enough, the expression contains PLANCK's elementary-length and even with  $\hbar$  according to our definition instead of  $h$ . If we now re-insert the values, we get:

$$S_b = 4\pi k \quad \text{for } L=0 \quad \text{as well as} \quad S_b = \pi k \quad \text{for } L=\hbar \quad (101)$$

Now we want to examine, whether the MLE actually owns a moment of momentum. We are based on our model (effective-value) developed in section 3.2. of [10]. For the moment of momentum  $\mathbf{L}$  applies generally:

$$\mathbf{L} = \mathbf{r} \times \mathbf{p} = m \cdot (\mathbf{r} \times \mathbf{v}) \quad (102)$$

With  $m=m_0$ ,  $r=r_0$ ,  $v=c$ ,  $c \perp r$  we get after application of (2) for the amount  $L$ :

$$L = m_0 c r_0 = \hbar \quad \text{and because of} \quad c = \omega_0 r_0 \quad (103)$$

$$W_0 = m_0 c^2 = \hbar \omega_0 \quad (104)$$

Expression (104) is apparently right. With it, we have explicitly proven, that the MLE owns a moment of momentum. It's equal to PLANCK's quantity of action i.e. as with a spin-2-particle or vice-versa:

*The PLANCK's quantity of action is defined by the effective-value of the moment of momentum of the MLE. The inherent moment of momentum (spin) is identical to the track moment of momentum.*

The last statement is justified by the fact that it's a matter of effective-value here. In reality,  $r_0$ ,  $m_0$  and the track- and inherent moment of momentum are temporally variable, nearly periodic functions. PLANCK's quantity of action is the sum of track- and inherent moment of momentum then. It's equal to  $\hbar$ , at which point one time the track-, the other time the inherent moment of momentum becomes zero. Such an interdependence even is called dualism. Naturally, PLANCK's quantity of action can be defined not only as moment of momentum. Another possibility is e.g.  $q_0\varphi_0$ . Because of GIBBS' fundamental equation the temperature of the MLE and with it of the whole metric wave field is equal to zero [8].

Going back to entropy. We see that the BOLTZMANN-constant figures an elementary quality of our metric fundamental lattice, as elementary as  $\varepsilon_0$ ,  $\mu_0$  and  $\kappa_0$ . Here, someone may say, this cannot be correct, since  $k$  is a purely statistical constant. Just we can answer this interjection: "The BOLTZMANN-constant is so elementary because it's statistical". Even  $\pi$  allows to be defined statistically.

### 3.2.2. Topology

We have determined the entropy of one discrete MLE. How does it look with a larger length then again? Since the single-entropy is a multiple of the BOLTZMANN-constant, we can calculate-on with the already known statistical relationships (95). In this connection the (absolute) maximum number of possible inner configurations within a volume with the radius  $r$  is given by the number of MLE's contained in this volume. With a cubic-face-centred crystal-lattice, the number within a cube with the edge length  $d$  is defined as:

$$N = 4 \left( \frac{d}{\rho} \right)^3 = 4 \left( \frac{d}{r_0} \right)^3 \quad (105)$$

$\rho$  is the lattice constant in this case. The fc-cube just contains 4 elements in total. Then, within a ball with the diameter  $d = \Lambda r_0$  and the volume  $\pi/6 d^3$  there are

$$N = \frac{2}{3} \pi \left( \frac{d}{\rho} \right)^3 = \frac{2}{3} \pi \left( \frac{\Lambda r_0}{r_0} \right)^3 = \frac{2}{3} \pi \Lambda^3 \quad (106)$$

individual MLE's. As long as  $\rho$  is not too large, we can insert (78) for  $\Lambda$ , otherwise (82):

$$N = \pi \tilde{Q}_0^3 \left( \left( 1 + \frac{t}{\tilde{T}} \right)^{\frac{1}{4}} \operatorname{artanh} \left( \left( 1 + \frac{t}{\tilde{T}} \right)^{-\frac{1}{4}} \left( \frac{2r}{\tilde{R}} \right)^{\frac{1}{3}} \right) - \left( \frac{2r}{\tilde{R}} \right)^{\frac{1}{3}} \right)^3 \quad \text{or} \quad (107)$$

$$N = \pi \tilde{Q}_0^3 \left( t^{\frac{1}{4}} \operatorname{artanh} \left( t^{-\frac{1}{4}} (2K_1 r)^{\frac{1}{3}} \right) - (2K_1 r)^{\frac{1}{3}} \right)^3 \quad \text{with } r = r/\tilde{R} \text{ and } K_1 = 1 \quad (108)$$

That's the number of elements within a sphere with the radius  $r$ . The course is shown in Figure 17 curve ①. If we insert the expression  $\Lambda_1 = \frac{3}{2} Q_0 \ln Q_0$  into (106), we obtain even a result for  $N_1$ . Here  $t \equiv 0$  reapplies. Then, the whole universe would contain altogether  $N_1 = \frac{9}{4} \pi Q_0^3 \ln^3 Q_0 = 1.13203 \cdot 10^{190}$  elements. Because of the propagation of the metric wave field this value is increasing continuously too (see Figure 19), and that according to  $N_1(T) = \frac{9}{4} \pi (\sqrt{bT})^3 \ln^3 \sqrt{bT}$  with  $b = 2 \kappa_0 / \varepsilon_0$ .

But for the calculation of the entropy  $S$  these values are sparsely helpful. As is known  $S$  is about a statistical value and (108) violates a basic rule of the statistics: *A value must not be counted repeatedly*. The relations (96ff) namely apply for a »normal« 3D-sphere only.

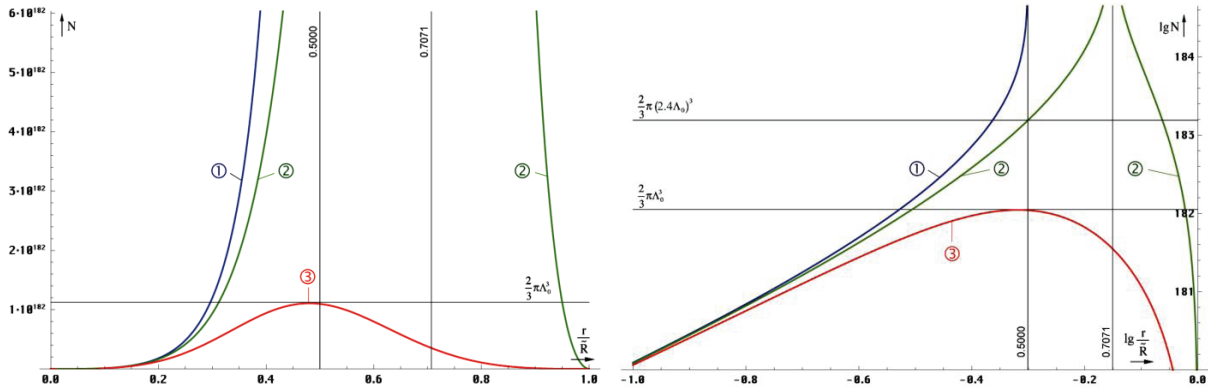


Figure 17  
Number of MLE's in dependence on the radius linear and logarithmic

But at the universe we have to take into account the particular 4D-topology. An observer in the free fall only imagines to be located in the spatial centre of the universe. In reality he is situated at a temporally singularity, the event horizon  $\{0,0,0,T\}$ . He is unable to overcome it, because beyond there is the future. Indeed, it's not about a point, but about a hyper-surface. All other observers at their own 3D-locations reside widespread at the same surface. Since T proceeds steadily, the temporal radius increases too and the observers are quasi »surfing« on the »time wave«. If one observer wants to visit another, he must accelerate. Thus, his temporally course is slowing down. Indeed, he does not travel to the past, but he is only »broken away« from the unbraked time lapse. He suddenly finds himself inside the sphere. With  $v=c$  the time stands still for him. Now he is situated at the real spatial centre, but only, because it came up to him.

That means, the spatial 4D-centre is not with the observer, but in the distance  $cT$  at the coordinates  $\{cT,cT,cT,0\}$ . More correct would be  $t_1$  instead of zero here. With the spatial centre it's also about a hyper-surface, a spatial singularity, the particle horizon. We cannot overcome even that. Like the temporal radius it's expanding steadily. Altogether it's about a closed system.

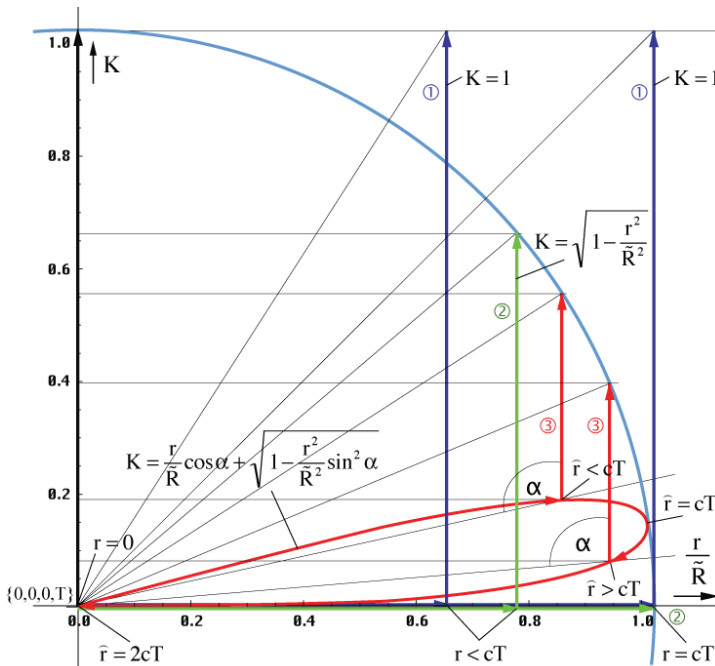


Figure 18  
Factor K in dependence on the radius for the 3 solutions (schematic presentation)

If two observers could swap their positions, they would find the same conditions on both locations. Since overall in the universe the same physical laws apply. Interesting thereat is, that we *observe* different conditions in a definite distance  $r$ .

The reason is the finite speed of light. The universe is *not* hot-wired, there is *no* instantaneous interconnection between whatever points (except for quantum entanglement).

For all observers the universe consists of the local conditions plus all forces and signals resulting from prior states, delayed by  $t \geq r/c$ . The farther, the elder the condition, that caused the impact.

And exactly that is the reason, why we cannot use expression (108). Approaching the distance  $cT$ , the MLE-density within  $\Lambda$  is in-cresing enormously indeed. But similarly, the universe

in that distance, at that time has had an essentially smaller world radius, a smaller surface. That means, the cross section must be smaller than at solution ①. *The larger* the distance  $r$ , *the smaller* the surface  $A$ , the opposite way around, as with a »normal« sphere.

Even e.g. the spherical shell in the distance  $R/2-r_1$  namely consists of only one single element. If its condition changes, it has a *simultaneous* effect on *all* vectors coming from *all* directions. But we are allowed to count only one element.

In fact that's good for MACH's principle, spatial damping cancels out, the strongest force is coming from the »edge«, but not for the statistics. That's why we are forced to find a function, which considers these special conditions. In doing so the reference to the time  $t$  should not get lost. Because I'm not a topology-expert, I tried to find such a function, at least roughly by introduction of a correction factor  $K$ ; the whole by trial and error. So it's not about a correct derivation here. With small  $r$  a possible solution should run similarly as with a 3D-sphere, likewise as solution ①. In the vicinity of  $R/2$  it should flatten out however. Either the border  $R/2$  should not be passed.

In addition to ① two more possible solutions are depicted in Figure 18 to the correction of one single coordinate. With solution ② (109) I assumed the volume of the inverse sphere to decrease with  $r$ . Solution ③ (110) additionally considers the curvature in the vicinity of  $R/2$  under consideration of the angle  $\alpha$ .

$$N = \pi \tilde{Q}_0^3 \left( t^{\frac{1}{4}} \operatorname{artanh} \left( t^{-\frac{1}{4}} (2K_2 r)^{\frac{1}{3}} \right) - (2K_2 r)^{\frac{1}{3}} \right)^3 \quad \text{with } K_2 = \sqrt{1-r^2} \quad (109)$$

$$N = \pi \tilde{Q}_0^3 \left( t^{\frac{1}{4}} \operatorname{artanh} \left( t^{-\frac{1}{4}} (2K_3 r)^{\frac{1}{3}} \right) - (2K_3 r)^{\frac{1}{3}} \right)^3 \quad \text{with } K_3 = r \cos \alpha + \sqrt{1-r^2 \sin^2 \alpha} \quad (110)$$

The angle  $\alpha(r)$  calculates as follows (*applies only in connection with (110)!!!*)

$$\alpha = \frac{\pi}{4} - \arg \left( -j4r \left( 1 - \left( \frac{H_2^{(1)}(r^{-1}/2)}{H_0^{(1)}(r^{-1}/2)} \right)^2 \right)^{-\frac{1}{2}} \right) \quad (111)$$

It's even only a rule of thumb. The course of both functions is depicted in Figure 18. As we can see, function (109) is less suitable, because it exceeds the  $R/2$ -border at  $N=2/3\pi(1.1955 \cdot Q_0)^3=2/3\pi(2.3909 \cdot \Lambda_0)^3$  – a crooked value. There isn't a flattening either, but a pole outside  $R/2$ .

Function (110) on the contrary fulfils all demands. It proceeds as with a 3D-sphere, like solution ① at small  $r$  and there is a flattening in the direct vicinity of  $R/2$ . Indeed, the function is defined beyond  $R/2$ , but without pole, and the value re-drops to zero at  $2cT$ . That means, it's about a time-like vector remaining inside the world radius. That's easy to understand. When rushing through the 4D-centre  $\{cT, cT, cT, 0\}$  or passing it within spitting distance, the vector re-approaches the observer and  $N$  has to decline again. The maximum is at the „magic“ value  $N_0=2/3\pi(Q_0/2)^3=2/3\pi\Lambda_0^3=1.51894 \cdot 10^{182}$ . The reason, why the function hits its maximum already on the verge of  $R/2$ , is its curvature. The arc-length becomes effective here.

By the way, all time-like vectors with the length  $2cT$ , regardless of continuous or discontinuous (virtual), are coming from a point with the coordinates  $\{r_1/2, r_1/2, r_1/2, t_1/4\}$ . That's behind the particle horizon, previous to the phase jump at  $Q=1$ , from a time, at which event- and particle-horizon still overlapped each other ( $Q=1/2$ ). The real world age is  $T$ , the length  $2cT$  is the result of curvature, propagation and expansion (see Figure 24).

Thus I'm sure, that (110) fits the actual conditions to the best. Then,  $N_0$  would be identical to the total number of possible micro-states of the universe and candidate for the calculation of the entropy  $S_0$ . The temporal dependence of  $N$  according to (110) for several constant

distances is depicted in Figure 19. The course of  $N_0(T)$  and  $N_1(T)$  in the comparison is shown top right. The rule of  $N_1$  has been scaled down about  $10^8$ , because both values gape apart too much.

Needless to say, the temporal functions are defined from  $N_0$  on only, above they are cropped. Solution ① proceeds similarly, but  $N_1$  is orders of magnitude greater, so that the crop takes place much higher in a range running nearly vertical up, which can no longer be processed by the plot program. And there is another difference. Distances  $>R/2$  aren't postponed into future with solution ① and ② similar to the dashed blue line (not to scale). That's correct. In contrast, solution ③ shows them, as if it's about a distance  $<R/2$ , which is also correct. Of course, there is even such a line with solution ③ (example  $0.8R'$ ), but it's not being emulated by expression (110). That's correct too, since there is a nearly infinite number of solutions already in the example range  $0.5\dots0.8R$  and beyond, depending on  $R'$ .

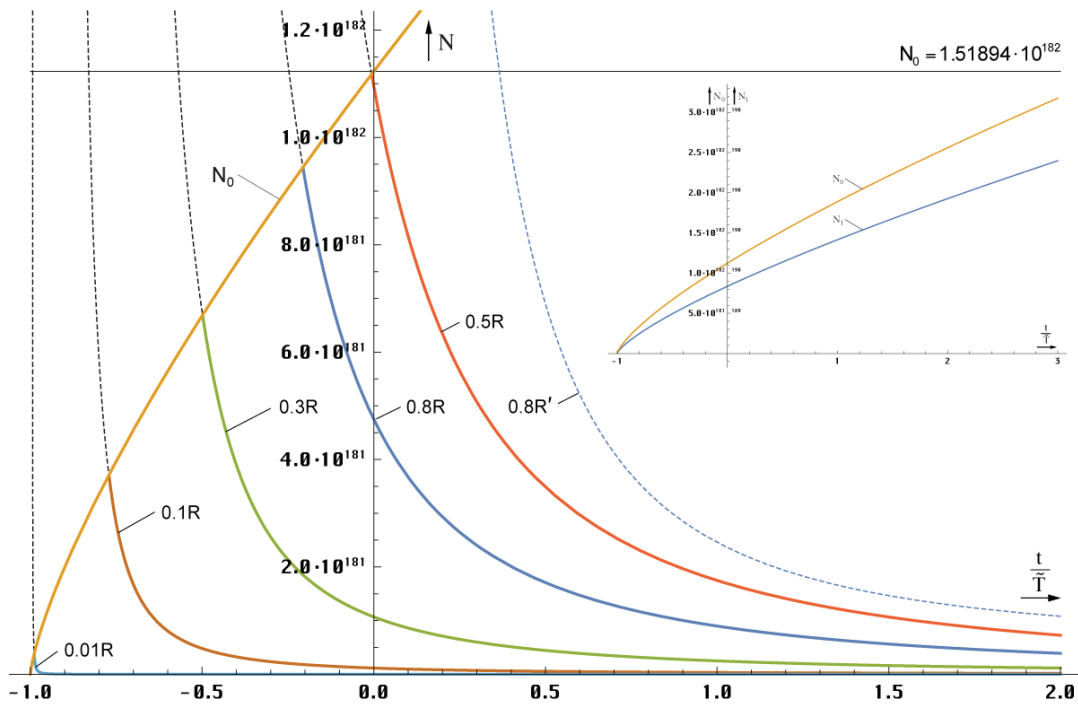


Figure 19  
Number of MLEs in dependence on time  
according to solution ③

### 3.2.3. Entropy

Now let's get down to the entropy. Generally (95) applies here. As determined more above, the entropy of the MLE calculates similar to that of a black hole according to (101) right ( $S_b$ ). Thus, we have to multiply (95) with  $\pi$ . However, that applies to the metric wave field only and not to the CMBR. All other problems may be calculated with the conventional ansatz and (95). In doubt just divide the results by  $\pi$ .

The course of the entropy  $S$  in dependence on the radius is shown in figure 48. Starting with a value of  $\pi k = 4.337465 \cdot 10^{-23} \text{JK}^{-1}$  with  $r=r_0$  the entropy ① rises continuously with increasing  $r$ , runs through a phase of minor ascend and skyrockets towards infinite with  $r \rightarrow cT$ . But an infinite value will not be achieved, since the number of line elements until the edge is limited to  $S_1(\Lambda_1)$ .

Because of the pole solution ② is less suitable. For solution ① we obtain the huge value of  $S_1 = 3\pi k (\frac{2}{3} + \ln Q_0 + \ln \ln Q_0) \approx 1312k = 1.89832 \cdot 10^{-20} \text{JK}^{-1}$ . For solution ③ the entropy  $S_0$  applies. It's defined as follows:

$$S_0 = \pi k \ln\left(\frac{2}{3} \pi \Lambda_0^3\right) = \pi k \ln\left(\frac{1}{12} \pi \tilde{Q}_0^3\right) = 1.81950 \cdot 10^{-20} \text{JK}^{-1} \quad (112)$$

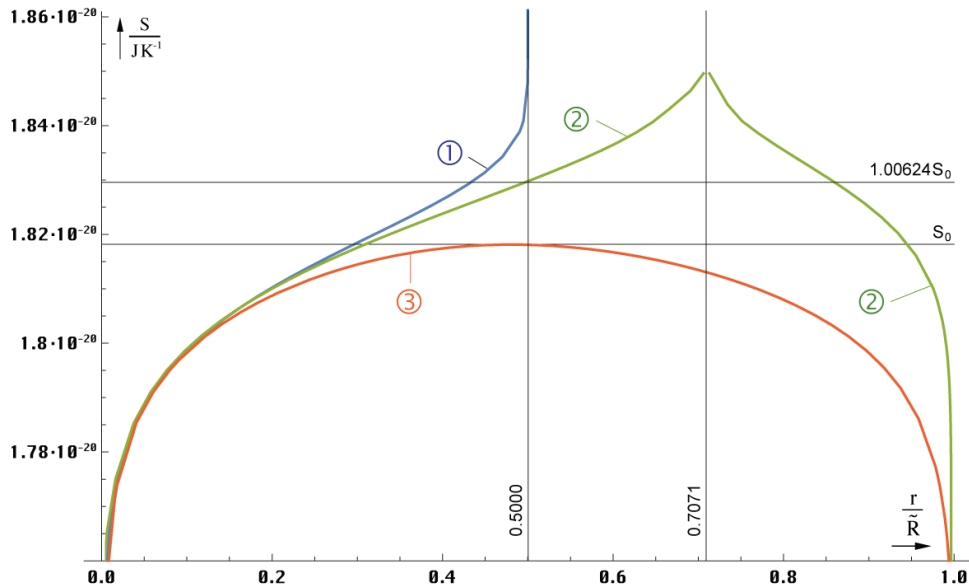


Figure 20  
Entropy in dependence on the radius

The temporal dependence of  $S_0$  for the case  $r=\text{const}$  is depicted in Figure 21. Interestingly enough the values of regions with fixed size decrease steadily. Maybe that's the »motor« of the evolution from the lower to the higher. In the case constant wave count vector the entropy  $S(r \neq R/2)$  remains constant across the whole definition range. It calculates according to (113) on the left. For  $S_0$  the right expression applies:

$$S = \pi k \ln N \qquad S_0 = \tilde{S}_0 + 6\pi k \ln t = \tilde{S}_0 + 3\pi k \ln \left( 1 + \frac{t}{\tilde{T}} \right) \qquad (113)$$

To calculate  $S_1$  we advantageously substitute  $Q_0$  with  $\tilde{Q}_0 t^2$  in the expression in the paragraph below figure 48. The entropy with constant wave count vector isn't defined across all times for all radii either. Certain distances don't exist, until the radius of the expanding universe has reached that length. Then  $S$  gets the value  $S_0$  resp.  $S_1$  exactly on entry. It applies: The later the entry, the higher starting entropy. Curves are being cropped even here in turn. Solution ① looks similar like Figure 21. The curve  $S_1$  proceeds far beyond the plot however. Initial distances  $> R/2$  are moved into future too, with solution ③ into the range  $< R/2$ , just like with  $N_1$  and  $N_0$ .

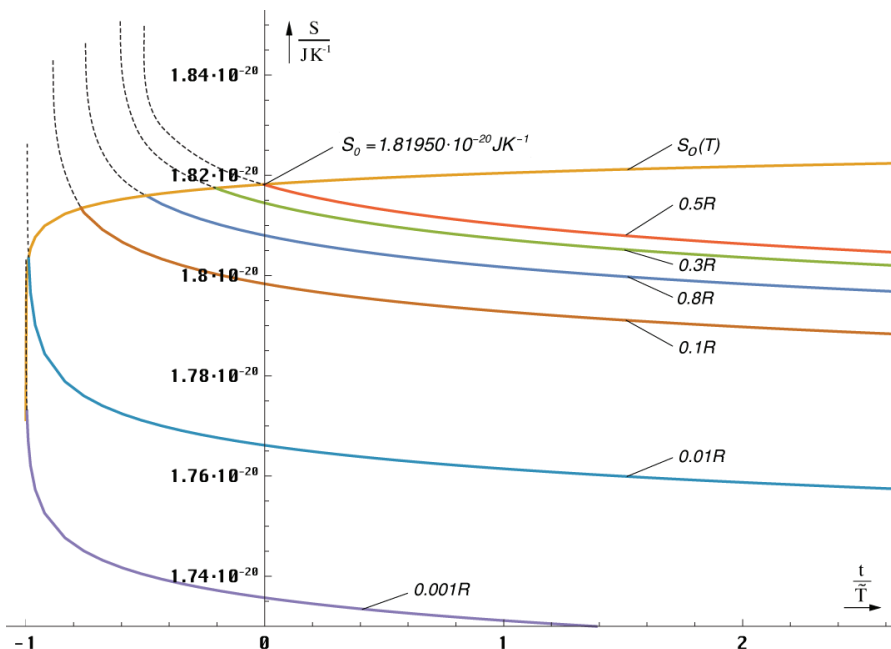


Figure 21  
Temporal dependence of the entropy for  $r=\text{const}$  (linear scale)



The temporal functions  $S_0$  and  $S_1$  are tending to  $\infty$ , as we can easily see by application of the limit theorems. Concerning the future of the universe we can say, that we don't have to fear a heat death. A thermodynamic equilibrium will never occur. The reason is the propagation of the metric wave field, as well as the expansion of the universe. That was a close shave!

## 4. Horizons of the universe

### 4.1. Particle horizon

As shown in section 3.2.1. the MLE disposes of an inner SCHWARZSCHILD-radius with the value  $r_{\pm}=r_0$ . It has the property of a particle horizon. Because of the relations  $R=r_0Q_0$  and  $r_1=r_0/Q_0$  it may be possible, that such a particle horizon also exists on a macroscopic scale, for the cosmos as a whole. The HUBBLE-parameter  $H_0=\omega_0Q_0^{-1}$  has the character of an angular frequency, just as  $\omega_0=\omega_1Q_0^{-1}$ . Thus, it may be possible, that even the whole universe owns an angular momentum in the amount of  $\hbar_1=\hbar Q_0$ . The MLE with its spin 2 lets suppose, that the universe also owns a spin of the size 2. That would explain a lot of phenomena. Therefore, with this information, we want to try, to calculate such a hypothetic SCHWARZSCHILD-radius  $R_{\pm}$  with ( $L=\hbar_1=\hbar Q_0$ ).

We start, in that we multiply (99) with  $Q_0$  resetting the bracketed expression to the definition  $a=\hbar m^{-1}c^{-1}$ . The value  $M_1$  is determined using the right-hand ansatz and (868 [10]):

$$R_{\pm} = Q_0 r_{\pm} = R \pm \sqrt{R^2 - \left(\frac{Q_0 \hbar_1}{2M_1 c}\right)^2} \quad \text{with} \quad \frac{M_1 G}{c^2} = 2ct \quad \left| \quad M_1 = m_0 Q_0 = \mu_0 \kappa_0 \hbar \quad (114)$$

$$R_{\pm} = R \pm \sqrt{R^2 - Q_0^2 r_0^2} = R \pm \sqrt{R^2 - R^2} = R \quad (115)$$

As result a double solution with  $R_{\pm}=R$  turns out, exactly as with the MLE but on a larger scale. The universe inside is larger then outside apparently, maybe due to the curvature of the time-like vectors. Interesting is the value  $M_1=1.81525 \cdot 10^{33}$  kg with  $H_0=68.6241$  kms<sup>-1</sup>Mpc<sup>-1</sup>. That's the total mass of the metric wave field and identical to MACH's counter mass. Dividing it by the volume  $V_1=4/3 \pi R^3$  we obtain a value of  $1.76907 \cdot 10^{-29}$  kg dm<sup>-3</sup> for the density. This one is exactly 3/2 times greater than the value  $G_{11}(R/2)$  calculated in section 7.2.7.2. of [10]. Well, we are living in a black hole actually and we can use nearly 100% thereof. Or is there yet an »outside« and the universe is nothing other than a huge line element?

### 4.2. Event horizon

That's the point or better the hyper-surface the observer (we) are living at. In reality it's not a point in space but a point in time: *The Present*. That means, it cannot be overcome because behind there is: *The Future*. Furthermore we must remark that we always assumed the expansion-centre as basis of the coordinate-system for the previous contemplations, where actually no length is defined. More essential qualities result from it for the two singular points.

*For the spatial singularity (expansion-centre) applies: Each length, measured from this point, always has the quantity  $R/2$ . Each period, measured at this point, always has the amount  $T$ , each frequency  $2H$ . It's about an event-horizon. It's a drain of the electromagnetic field. To the approximation applies  $r=\infty$ ,  $t=\infty$ .*

*For the temporal singularity (wave-front) applies: Each length, measured from this point, always has the quantity  $r_1/2$ . Each period, measured at this point, always has the amount  $t_1$ , each frequency  $2\omega_1$ . It's about a particle-horizon. It's a source of the electromagnetic field. To the approximation applies  $r=0, t=0$ .*

A particle horizon on the inside is an event horizon on the outside and vice versa. It looks similar to the magnetic and electric fields. No matter at which pole you are located, you always believe that you are at the centre, since all field lines always converge rectangularly to

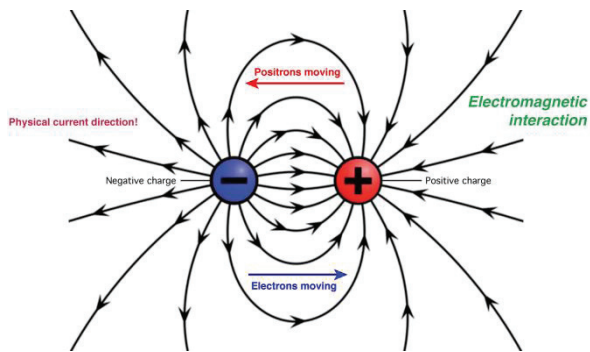


Figure 22  
Poles and field lines in the electrical field [12]

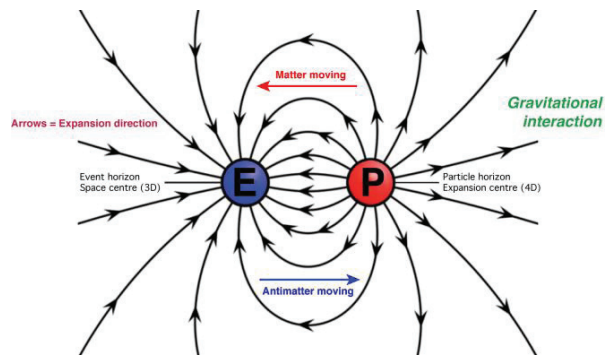


Figure 23  
Horizons and field lines in the gravity field

the observer from all directions (Figure 23). Except that he is unable to really reach the particle horizon. I can't say whether the two poles are connected in the background like with the horseshoe magnet. In any case, there is more than only one event horizon, once for the universe as a whole, as well as a huge number what with black holes.

## 5. Distance-vectors

Due to the progress in the technical domain taken place in the most recent time, the astronomers are able to look into the universe deeper and deeper and with it even farther back in time. The farther one looks however, all the more the structure of the universe becomes notably and must be taken into consideration on the interpretation of the measuring results. Otherwise the much money would have been poured down the drain.

But before expanding further, just let's have a look at a so simple quantity, like the distance respectively the spacing to a stellar object. The astronomer just sits in front of his telescope, observing an object and he tries to determine with different methods, how far away it is. And before he can determine the HUBBLE-parameter, he must determine the distance respectively the spacing to the object of course. And the first problem already appears here: What do we actually mean by distance as well as spacing? And what do we really want to determine?

In the close-up range this question can be answered relatively simply: The spacing is equal to the distance and the light from the object has covered this, when it has arrived at the observer. But if we leave the close-up range, looking at objects farther away, it's no longer like this. At first, we look at the object by means of photons, which have moved from the object into our direction. Thus, in reference to the metrics, it's about an (incoming) time-like vector (Figure 24 and 22  $r_T$  red pictured), a negative distance. We call it *time-like distance*. It corresponds to the constant wave count vector of the metrics. On this occasion, we how-ever actually observe the zero vector and not the time-like vector. With vanishing curvature both coincides indeed. As it looks like, when there is a curvature, will be presented later.

But the object, we observe nowadays, is already located at a completely different position, as our observation-data want to make believe, since these are already totally »outdated«,



when they reach us. One feature of this model is now, that this is not the case. Even when the signals are already very old, the object really resides in reference to the observer's  $R^4$ -coordinate-system at that very position, where he observes it. The length of the vector from the object to the observer however cannot be influenced by him, because he is just only observer.

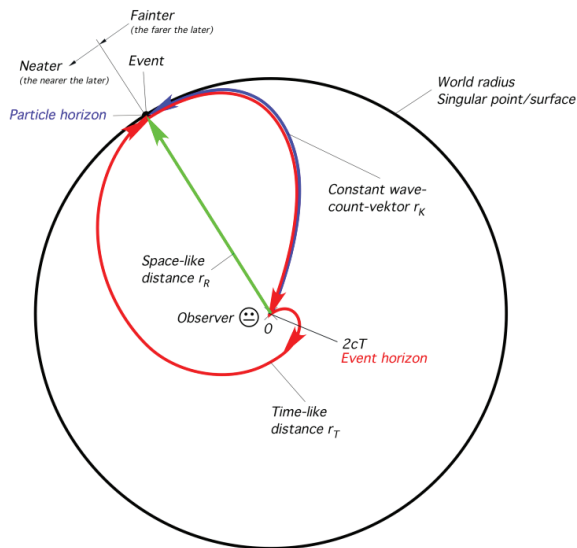


Figure 24  
Distance-vectors with an object  
at the edge of the universe (schematized)

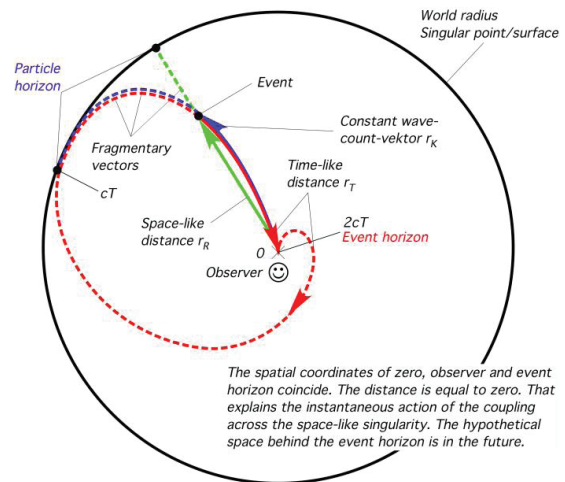


Figure 25  
Distance-vectors with an object  
in the close-up range of the observer (schematized)

But if the observer has the intent, to visit the object, that would be an (outgoing) space-like vector then, a positive distance/spacing, this cannot take place on the same way, which the ray of light has covered, because the observer would have to move with  $c$  thereto and each zero vector is unique. Now, another distance/spacing is applied to him.

To the difference between *distance* and *spacing*: These are (approximately) equal in the close-up range only. With larger distances, objects in the free fall move away from each other according to the distance-function with constant wave count vector. That would be the real *spacing* ( $r_K$  blue pictured). With it, also the definition of the *space-like distance* turns out ( $r_R$  green pictured). This is the shortest way between the observer or better the traveller and the object. It is an imagined line and coincides with the coordinate  $r$  of the coordinate-system. Locally, it is equal to the space-like vector of the metrics.

1. The *zero vector*  $r_N$  is the way a ray of light covers, at which point the velocity in reference to the subspace is  $c$  constantly. In the local range it is equal to the geometrical sum of space- and time-like vector.
2. The *time-like distance*  $r_T$  is the way a ray of light, starting from the source, has covered, when it has been arrived at the observer. In the local range, it corresponds to the time-like vector of the metrics. But actually the zero vector  $r_N$  is observed.
3. The *spacing*  $r_K$  is the distance between two objects in the free fall. The vector proceeds along the field-lines of the gravitational-field and varies according to the spacing-function with constant wave count vector. It corresponds to the zero vector  $r_N$  of the metrics.
4. The *space-like distance*  $r_R$  is the shortest vector between a traveller and his destination. It's about an imagined line. It is identical to the coordinate  $r$  of the coordinate-system. In the local range, it corresponds to the space-like vector of the metrics. If one wants to travel along this line, permanent navigation (acceleration) is needed.

But this way, the destination cannot be reached in the free fall, as an analogy from the navigation suggests – the difference between latitudinal and great-circle-distance. When start

and destination are on the same latitude and if it's not exactly about the equator, the great-circle-distance is always smaller than the latitudinal-circle-distance. During great-circle-navigation however, the captain must change the course continually, just accelerate, whereas he could theoretically continue his journey without acceleration on the latitudinal circle, just in the free fall, when the water resistance would be zero. Thus, the voyager has the chance, to influence the distance, namely by means of navigation. To the better overview the definitions once again:

But let's descend to *the time-like distance* once again. This is the distance, the astronomer determines, when he analyzes incoming light- or radio-signals (zero vectors). They are subject to a red-shift according to the propagation-function in section 4.3.4.4.3. resp. 5.3.2. of [10]. The *time-like distance* is limited to the maximum *time-like distance*, which results from the Total-Age  $2T$ . It applies  $r_{T\max} = R = 2cT$ .

All these vectors are coming from the same point  $\{r_1, r_1, r_1, 2t_1\}$  and are ending at all points of the hyper-surface  $\{R, R, R, 2T\}$  at the same time. Both are superimposed for any observer. The point  $\{r_1, r_1, r_1, 2t_1\}$  is quasi „smeared“ across the whole universe, i.e. all points on the hyper-surface are interconnected via  $\{r_1, r_1, r_1, 2t_1\}$  and, since photons are timeless, even instantaneously. That may be the cause for such effects like quantum entanglement etc.

In the course of this work, we had learned that the maximum *space-like distance* amounts to only the half of it:  $r_{R\max} = R/2 = cT$ . It would be interesting if we were able to convert the above values into one another. First of all, expression (116) would be suitable for this:

$$r_T = -\frac{r_R}{\sqrt{1 - \frac{4r_R^2}{R^2}}} \quad r_R = -\frac{r_T}{\sqrt{1 + \frac{4r_T^2}{R^2}}} \quad (116)$$

Considering the two expressions now, one recognizes that these fail at the »edge« of the universe. The left-hand expression submits a negative infinite *time-like distance* for  $R/2$ , the right-hand expression a *space-like distance* of  $0.447214R = 0.894427cT$  for  $-R/2$ . Actually, a value of  $0.5R = cT$  should arise however. In addition, since  $r_T$  returns to its starting point over time, there should be a second solution for the left expression.

With the *time-like vector* we must pay attention to the following: This can be both, an incoming (negative distance), as well as an outgoing vector (positive distance). An observer always is concerned with an incoming vector, whose length is limited to  $-2cT$ . The light has traversed the entire universe then and has been rearrived at it's starting point, a space-like singularity (event horizon). The farthest ( $r_R$ ) starting point of an incoming time-like vector is in the distance  $-cT$ . The maximum length of an outgoing time-like vector on the other hand is unlimited because it directs to future. Of course, it is even subject to the parametric attenuation. It's impossible to send signals back in time.

Of particular interest are the signals directly from the Big Bang  $-2T$ . These have reached their starting point again and are to be observed as cosmologic background-radiation, although with extreme red-shift. The picture, which it generates, is really the view of the point of observer to the point of time  $-2T$ , however mirror-inverted in all four dimensions (an outgoing time-like vector becomes an incoming one). The range between  $-2T$  and  $-T$  is also accessible indeed, but these signals come from areas at the opposite end, with a lower distance than  $-R/2$ , at which point the signal is coming „from behind“ on a detour. In this case applies, the older the signal, the nearer the source (neater).

With it, both expressions are been suitable only conditionally for the calculation of problems involving the universe as a whole. For further considerations we need the correct expression

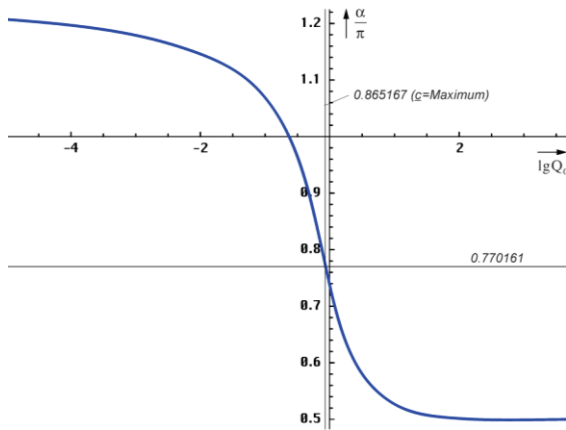


Figure 26  
Angle  $\alpha$  as a function of  $Q_0$

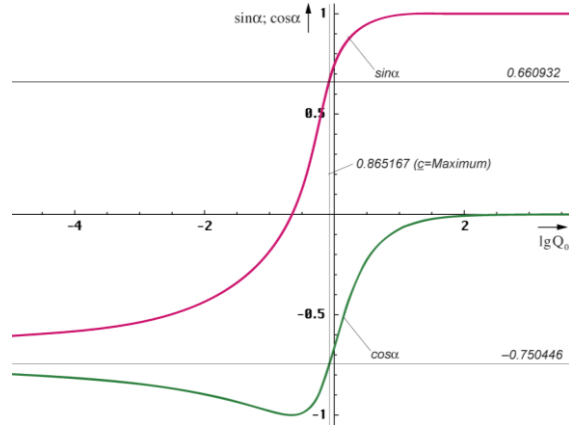


Figure 27  
Functions  $\sin \alpha$  and  $\cos \alpha$  as a function of  $Q_0$

considering the angle  $\alpha$ . It can be determined with the help of (30) as a function of  $Q$ . Since  $Q$  in turn depends on the distance  $r$ , it has the value  $Q_0$  at the observer, at the distance  $R/2$  it is equal to one, we need a function  $Qr=Q(r)$ . We get it by rearranging (895 [10]) to (117), since  $r$  is oriented in the opposite direction in this case.

The expression  $\sqrt{-g_{00}}$  is only effective at a microscopic distance from  $R/2$ , so it can be neglected. We apply  $Q_0$  for  $Q_{\max}$ , which we assume to be pretty much the maximum value (844 [10]). I chose this form in order to be able to calculate the course even for other reference frames and to create equality with the RhoQ function. The course of  $\alpha$  as a function of  $Q_0$  is depicted in Figure 153 and 146.

Now we come to the actual calculation. However, only the function  $r_R(r_T)$  can be presented explicitly.

$$Q(r) = \frac{\tilde{Q}_0}{Q_{\max}} \frac{\tilde{R}}{2r} \quad (117)$$

```

Qr = Function[#1/Q0/2/#2];
PhiQ = Function[If[# > 10^4, -Pi/4-3/4/#, Arg[1/Sqrt[1-(HankeIH1[2, #]/HankeIH1[0, #])^2]]- Pi/2]];
PhiR = Function[PhiQ[Qr[#1, #2]]];
AlphaR = Function[N[Pi/4 - PhiR[#1, #2]]];

```

$$r_R = -r_T \left( \frac{r_T}{R} \cos \alpha(r_T) + \sqrt{1 - \left( \frac{r_T}{R} \right)^2 \sin^2 \alpha(r_T)} \right)^{\frac{1}{3}} \quad (118)$$

```

rtrr = Function[# (# Cos[AlphaR[Q0, #]] + Sqrt[1 - #^2 Sin[AlphaR[Q0, #]]^2])^(1/3)];

```

I determined expression (118) based on (110) in combination with (698 [10]). There was already a similar problem with the calculation of entropy. The inverse functions  $r_{T1}$  (RTR1) and  $r_{T2}$  (RTR2) we obtain with the help of Interpolation[list] by calculating  $r_R(r_T)$  and swapping the x and y values in the list of support points:

```

inrt1={};
For[d=0.001; i=0,d<.739,(++i),d+=.001; AppendTo[inrt1,{rtrr[d],d}]]
inrt2={};
For[d=0.739; i=0,d<.999,(++i),d+=.001; AppendTo[inrt2,{rtrr[d],d}]]
RTRR1=Interpolation[inrt1];
RTRR2=Interpolation[inrt2];
RTR1=Function[If[#<=0.49034 ,RTRR1[#,Null]]];
RTR2=Function[If[#<=0.49034 ,RTRR2[#,Null]]];

```

For the constant wave count vector  $r_K$  we obtain:

$$r_R = r_K \left( 1 - \left( \frac{3}{4} \frac{r_K}{R} \right)^2 \right)^{\frac{2}{3}} \quad (120)$$

**rkrr = Function[# (1 - (3/4 #)^2)^(2/3)];**

The factor  $\frac{3}{4}$  results from our finding that the HUBBLE-parameter  $H_1$  has the value  $\frac{3}{4}T^{-1}$  at the edge of the universe in contrast to the local value  $H_0 = \frac{1}{2}T^{-1}$ . Or rather, the entire distance between the observer and  $R/2$  expands with the exponent  $\frac{3}{4}$  with respect to  $T$ . With  $H_0 = \frac{1}{2}T^{-1}$ ,  $r_K$  would not reach the edge at  $R/2$  at all and would take an earlier »turn«. Even with  $r_K$  the inverse function can be defined using the function `Interpolation[list]` only. Since  $r_K$  points away from the observer, we don't need it either. The course of the above mentioned functions is shown in Figure 28.

It can be seen that all three vectors coincide at close range and far beyond. At a distance of e.g. 400 Mpc, the deviation between  $r_R$  and  $r_T$  is only 2% and thus far below the observation error. The function  $r_T$  does not leave the universe, which is correct, but it does not reach  $R/2$  either, but is redirected back to the starting point shortly before. With it, we are able to observe 94.31% of the universe.

The faster expansion just after the BB is also taken into account. The turning point, i.e. the greatest distance, is already reached in the first third. Thus, expression (118) fulfils the requirements placed on it. But what's about  $r_K$ ? Because of  $H_1 = \frac{3}{4}T^{-1}$  the edge at  $R/2$  is reached and passed with the angle  $\varphi$ , see Figure 16 and Figure 29. The space beyond is in the future of the observer.

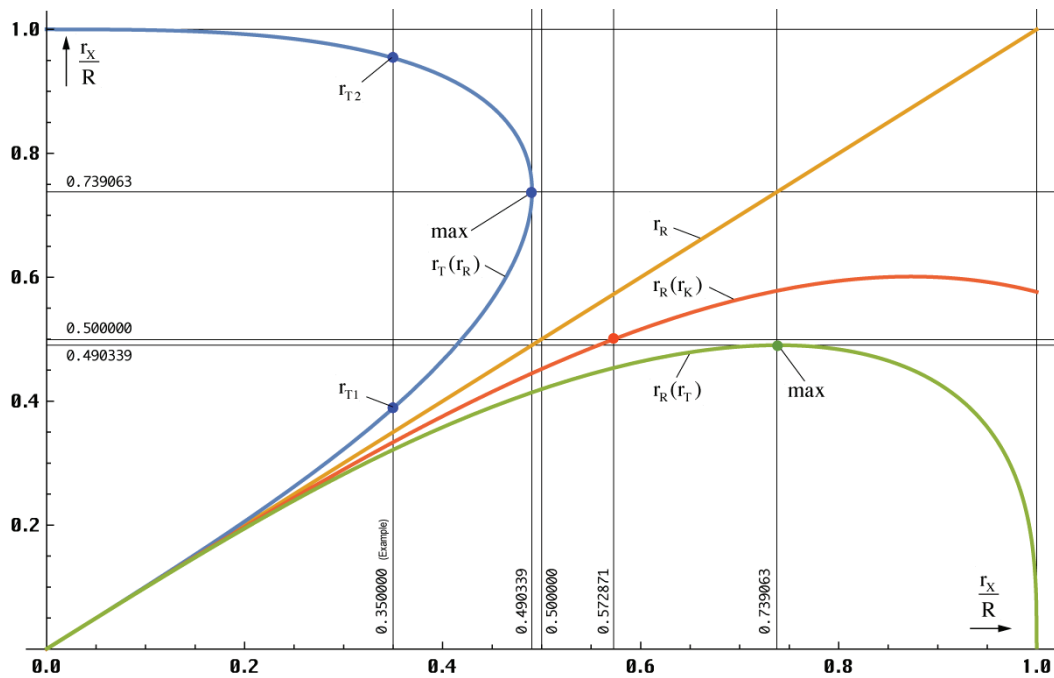


Figure 28  
Distance-vectors in the universe (1D)

Figure 28 was created using the following program:

```
GH=Function[Graphics[Line[{{#2,#1},{#3,#1}}]]];
GU=Function[Graphics[Line[{{#1,#2},{#1,#3}}]]];
x01=.35 (* The example distance *);
y02=FindMaximum[rtrr[r], {r,.5,.8}]
y2=First[y02];
x2=r/.First[Rest[y02]];
y03=FindMaximum[rkrr[r], {r,.5,.8}]
y3=First[y03];
x3=r/.First[Rest[y03]];
z3=xx/.FindRoot[R3[2Pi xx]-.5==0, {xx,0.5,.7}]
```

(121)

```

Plot[{RTR2[r]}, {r,0,1}, PlotRange->{0,1.03}, ImageSize->Large];
Plot[{RTR1[r], r, rtrr[r], rkrr[r]}, {r,0,1},
PlotRange->{0,1.03}, ImageSize->Large, PlotStyle->{Thickness[0.0038]};
Show[%, %, GH[y2,0,2], GH[1/2,0,2], GH[1,0,2], GH[x2,0,2],
GV[.5,-1,2], GV[x2,-1,2], GV[1,-1,2], GV[y2,-1,2], GV[x01,-1,2], GV[z3,-1,2],
Graphics[{PointSize[0.01], Blue, Point[{{x01,RTR1[x01]}, {x01,RTR2[x01]}]}],
Graphics[{PointSize[0.01], ColorData[1,12], Point[{x2,y2}]}],
Graphics[{PointSize[0.01], ColorData[2,2], Point[{z3,0.5}]}],
PlotLabel->„Blau Rt(Rr), Orange Rr(Rr), Grün Rr(Rt), Rot Rr(Rk)“,
LabelStyle->{FontFamily->„Chicago“,10,GrayLevel[0]}, ImageSize->Large]

```

Figure 29 shows the 2D-presentation  $r(T)$  in polar coordinates, whereat the time  $T$  is represented by the angle  $\vartheta$ . The observer is located at the point  $\{0,0\}$ . The Age  $2T$  equals to one complete revolution. Every observer always has the impression to be at the point  $2T$  (event horizon). That's correct. Therefore there is no continuation of  $r_K$  along the dashed black line. The vector  $r_R$  mutates to the generic logarithmic spiral.

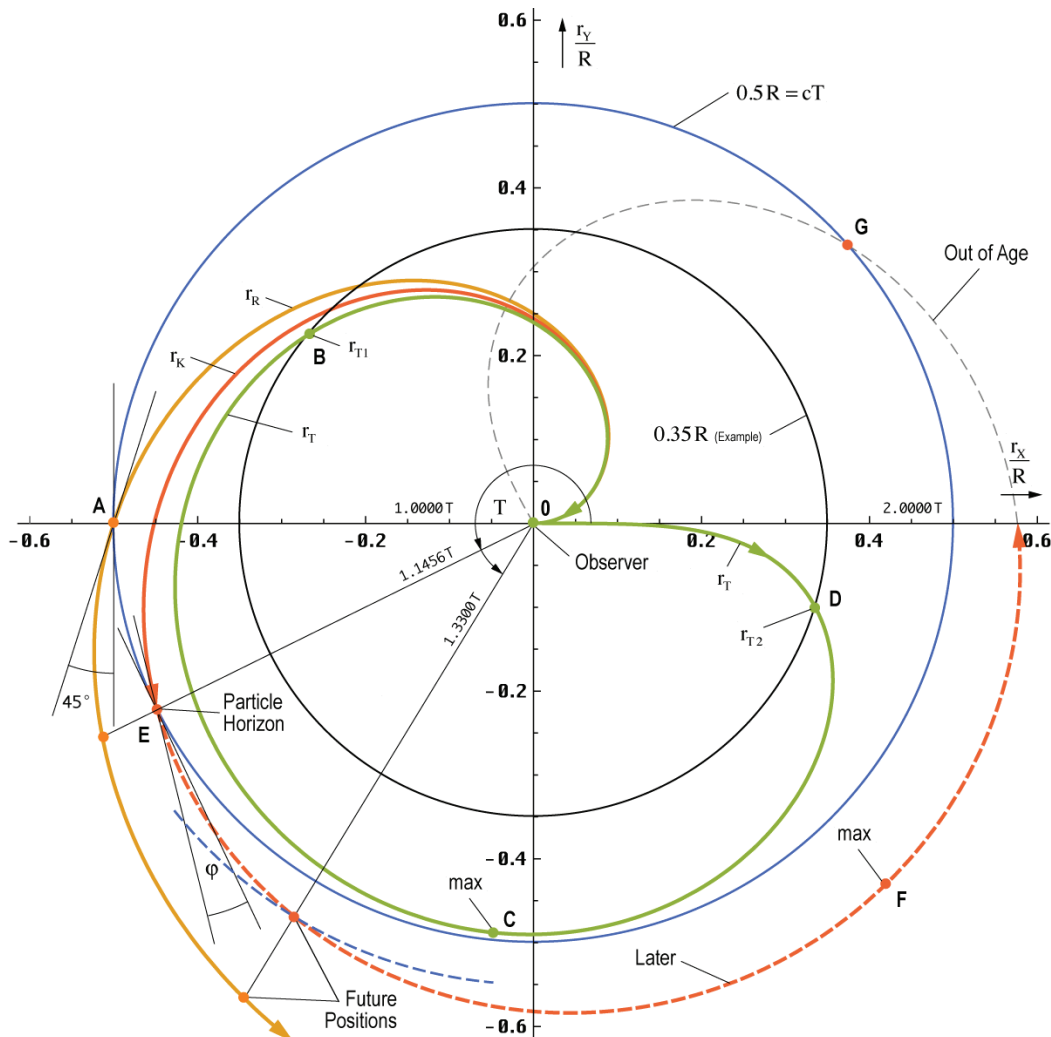


Figure 29  
2D-course of the distance-vectors  $r_R$ ,  $r_K$  and  $r_T$  as a function of time

Figure 29 has been created using the following program:

```

z31=r/.FindRoot[R3[r]-.5==0, {r,.1,.5}]
z32=r/.Chop[FindRoot[R3[r]-.5==0, {r,5,6}]]
z33=r/.First[Rest[FindMaximum[R3[r], {r,5,6}]]]
R2=Function[rtrr[#/2/Pi]];
R3=Function[rkrr[#/2/Pi]];

```

```

Plot[{Pi*r+Pi/2}, {r,-.6,-.45}, ImageSize->Large,
PlotRange->{-0.52,0.52}, PlotStyle->{Thickness[0.001],Black}, AspectRatio->1];
PolarPlot[Null,r/2/Pi,R2[r],R3[r], {r,0,8/3 Pi}, PlotRange->0.59,
ImageSize->Large,AspectRatio->1];

```

(122)

```
Show[%, %, GV[-0.5,-0.6,0.6],
Graphics[{Circle[{0,0},1], Circle[{0,0},0.5], Circle[{0,0},κ01]},
Graphics[{PointSize[0.01], Orange, Point[{-0.5,0}],
Graphics[{PointSize[0.01], Red, Point[{
{R3[z31]Cos[z31], R3[z31]Sin[z31]},
{R3[z32]Cos[z32], R3[z32]Sin[z32]},
{R3[z33]Cos[z33], R3[z33]Sin[z33]}]}]},
Graphics[{PointSize[0.01], ColorData[1,12], Point[{0,0},
{y2 Cos[2 Pi RTR1[y2]], y2 Sin[2 Pi RTR1[y2]],
{x01 Cos[2 Pi RTR1[x01]], x01 Sin[2 Pi RTR1[x01]],
{x01 Cos[2 Pi RTR2[x01]], x01 Sin[2 Pi RTR2[x01]}]}]},
LabelStyle->{FontFamily->"Chicago", 10, GrayLevel[0]}, ImageSize->Large]
```

The 2D-representation gives the impression that the incoming vector  $r_T$  is coming from the direction in which it was originally emitted. But that's not the case. In fact, he's coming from the opposite direction. This can be seen very well in the 3D-representation in Figure 30.

At this point we make use of the fact that  $H_0$  is an angular frequency. And for every observer, no matter in which reference system or where he is, the universe has always completed exactly one revolution around all three spatial axes. However, only two of them are shown in Figure 158, giving the impression that the maximum observable radius  $r_R$  is at the point C. However, the images arriving from one direction are actually from a circle of diameter  $0.490339R$  passing through point C. Therefore, an exact localization of the sources actual position is impossible.

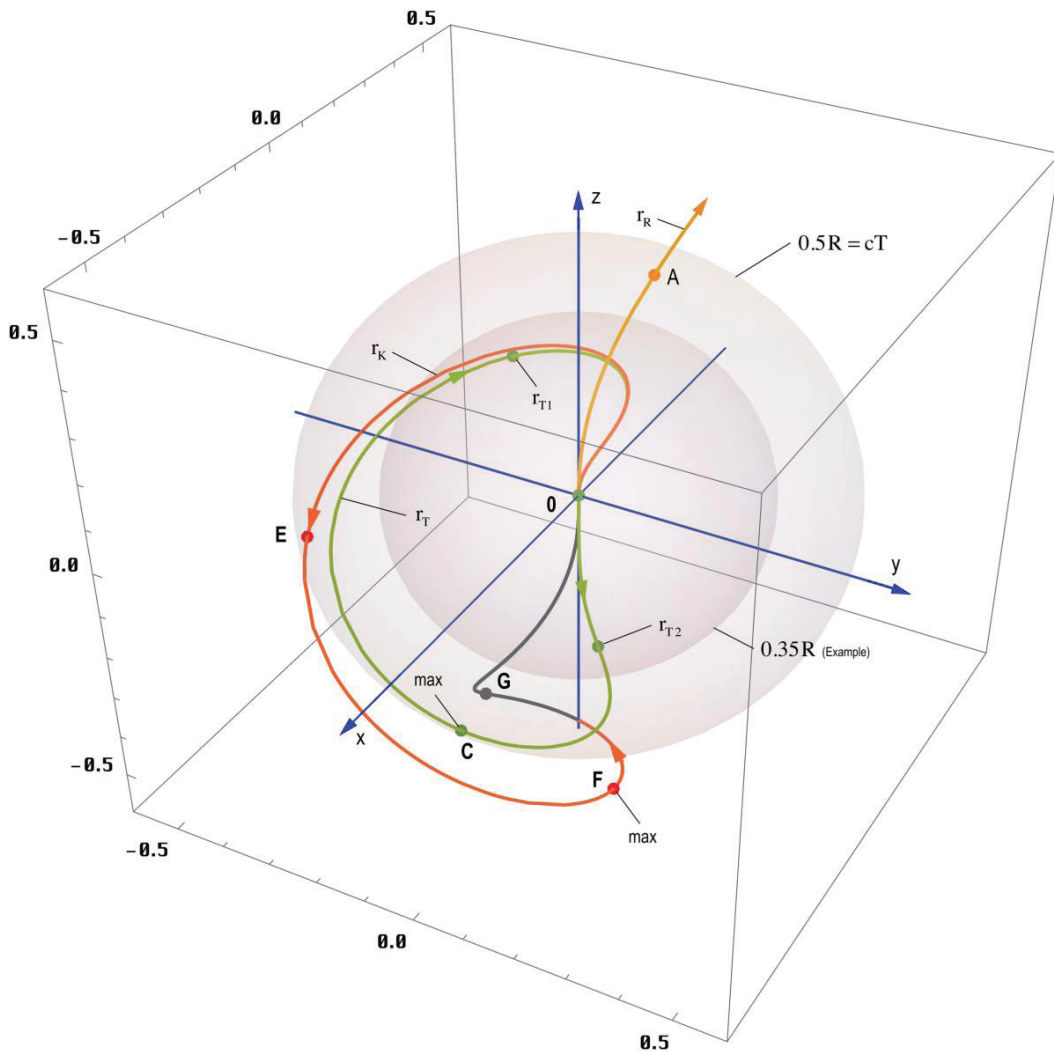


Figure 30  
3D-course of the distance-vectors  $r_R$ ,  $r_K$  and  $r_T$  as a function of time



But we can not only observe objects on this circle. Since it's about an  $R^4$ -universe, we have one additional degree of freedom left, which means, the circle also rotates about its diameter. With it, we are able to observe all objects within a sphere with the radius  $0.490339R$ , whereby the signals then arrive from the entire solid angle  $4\pi$ .

Figure 30 shows the example sphere and the  $R/2$  sphere. As in Figure 29, the extrema and the intersections are marked with coloured dots and letters. Unfortunately it was not possible to show the section D-F-z as a dashed line. One can also see that the vector  $r_R$  deviates extremely from  $r_K$  very early on, a challenge for navigation. Figure 30 has been created with the following program:

```

z1=Line[{{(0,0,-.7),(0,0,.7)},{(0,-.7,0),(0,.7,0)},{(-.7,0,0),(0.7,0,0)}}] (*Axes cross*);
ParametricPlot3D[{{(1,1,1), {r Cos[r]Sin[r/2], r Sin[r]Sin[r/2], r Cos[r/2]},
{R2[r]Cos[r]Sin[r/2],R2[r]Sin[r]Sin[r/2],R2[r]Cos[r/2]},
{R3[r]Cos[r]Sin[r/2],R3[r]Sin[r]Sin[r/2],R3[r]Cos[r/2]}},
{r,0,8/3 Pi}, PlotRange->0.6, ImageSize->Large, AspectRatio->1,
LabelStyle->{FontFamily->"Chicago",10,GrayLevel[0]}, ImageSize->Large];

Show[%,
Graphics3D[{Opacity[0.1], Sphere[{0,0,0}, 0.5]}],
Graphics3D[{Opacity[0.1], Sphere[{0,0,0}, κ01]}],
Graphics3D[{Thickness[0.0025], Blue,z1}],
Graphics3D[{PointSize[0.0125], Orange, Point[{
.5 Cos[.5]Sin[.25],.5 Sin[.5]Sin[.25],.5 Cos[.25]}]}],
Graphics3D[{PointSize[0.0125], Red, Point[{
{R3[z31]Cos[z31]Sin[z31/2],R3[z31]Sin[z31]Sin[z31/2],R3[z31]Cos[z31/2]},
{R3[z32]Cos[z32]Sin[z32/2],R3[z32]Sin[z32]Sin[z32/2],R3[z32]Cos[z32/2]},
{R3[z33]Cos[z33]Sin[z33/2],R3[z33]Sin[z33]Sin[z33/2],R3[z33]Cos[z33/2]}]}],
Graphics3D[{{PointSize[0.0125],ColorData[1,12],Point[{{(0,0,0),
{y2 Cos[2 Pi RTR1[y2]]Sin[Pi RTR1[y2]],y2 Sin[2 Pi RTR1[y2]]Sin[Pi RTR1[y2]], y2 Cos[Pi RTR1[y2]]},
{κ01 Cos[2 Pi RTR1[κ01]]Sin[Pi RTR1[κ01]],
κ01 Sin[2 Pi RTR1[κ01]]Sin[Pi RTR1[κ01]],
κ01 Cos[Pi RTR1[κ01]],
{κ01 Cos[2 Pi RTR2[κ01]]Sin[Pi RTR2[κ01]],
κ01 Sin[2 Pi RTR2[κ01]]Sin[Pi RTR2[κ01]],
κ01 Cos[Pi RTR2[κ01]] }]}]}]]

```

But there is an additional way of presentation. If we replace the temporal dimension by the third spatial one, we can let rotate the  $r_T$ -curve obtaining a body of revolution with interesting properties:

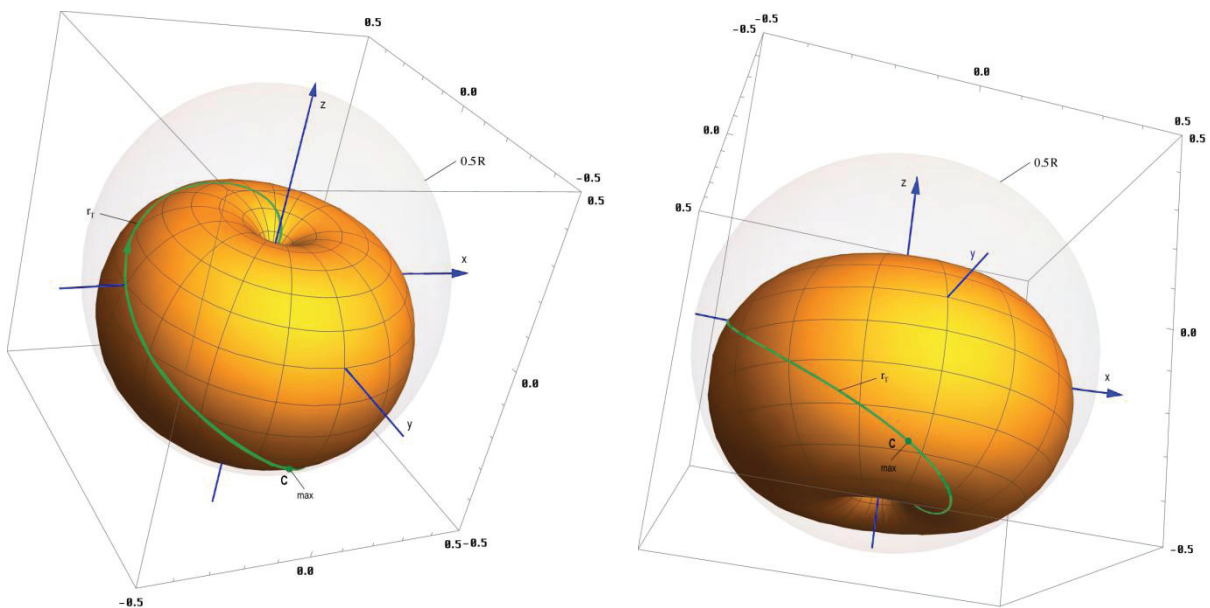


Figure 31  
Possible shape of the electron  
and/or of the PLANCK charge

The representation is similar to Figure 8 in [10], which would close the circle. The model has the property of logarithmic periodicity, i.e. there are similarities between the microcosm and the macrocosm.

My assumption is therefore that the object in Figure 31 could be identical to the PLANCK's charge and/or the electron, as its freely occurring form, just on a different scale. Instead of rotating with  $H_0$  it would rotate with  $\omega_0$  then and a part of the charge would reside in the interior, so that the observable part would depend on the viewing angle. This would also explain the need to correct  $r_e$ . Then, the electron would be the 3D-manifestation of a 4D-object. But as I said, this is just a guess on my part. The object can be displayed with the following program:

```
P11=ParametricPlot3D[{{R2[r]Cos[s]Sin[r/2],R2[r]Sin[s]Sin[r/2],R2[r]Cos[r/2]}},
{r,0,2 Pi}, {s,0,2 Pi}, PlotRange->0.5, ImageSize->Large,
PlotStyle->{Opacity[1],FillingStyle->Opacity[0.1]}, AspectRatio->1,
LabelStyle->{FontFamily->"Chicago",10,GrayLevel[0]}];

P12=ParametricPlot3D[{{R2[r]Cos[r]Sin[r/2],R2[r]Sin[r]Sin[r/2],R2[r]Cos[r/2]}},
{r,0,2 Pi}, PlotRange->0.5, ImageSize->Large, AspectRatio->1,
PlotStyle->{ColorData[1,8],Thickness[0.005]},
LabelStyle->{FontFamily->"Chicago",10,GrayLevel[0]}];

Show[P12, P11, Graphics3D[{Opacity[0.075], Sphere[{0,0,0},0.5]}],
Graphics3D[{Thickness[0.0025],Blue,z1}],
Graphics3D[{{PointSize[0.013],ColorData[1,8], Point[{{0,0,0},
{y2 Cos[2 Pi RTR1[y2]]Sin[Pi RTR1[y2]],y2 Sin[2 Pi RTR1[y2]]Sin[Pi RTR1[y2]],
y2 Cos[Pi RTR1[y2]] }]}]}]]
```

(125)

## 6. Summary

In the course of this work, with the help of the model from [10], we succeeded in the definition of the propagation function of the metric wave field, postulated by LANCZOS. That, on the other hand, was the base for the determination of the HUBBLE-parameter for greater distances. It was shown, that this depends on the initial distance. The exact function could be determined. Furthermore the entropy of the metric wave field was determined — under consideration of the special 4D-topology of the universe. Its value will increase steadily even in future and there is no fear of a heath death anyway. The reason is the expansion of the universe, the propagation of the metric wave field and the curvature of the constant wave count vector in turn.

## 7. The Concerted International System of Units

A variety of formulas for the calculation of various variables and graphics are specified in the course of this work. These in turn access certain values and natural constants whose meaning or values are not shown in the text, but which are required to carry out the calculations correctly.

Using the MLE model of [10] it has been possible to calculate a series of natural constants associated with the electron, the proton and the  $^1\text{H}$  atom via their relation to the reference frame  $Q_0$  and that exactly. The model is based on the basic variables of the subspace, which are fixed values, independent of the reference system. It is sufficient to define only five genuine constants ( $\mu_0$ ,  $c$ ,  $\kappa_0$ ,  $\hbar_1$  and  $k$ ) as base variables plus a so-called *Magic value*, in this case  $m_e$  to specify the reference system  $Q_0$ . All values are related via  $Q_0$ ; if one value changes, they all change. If an influence is added, it is yet another reference system. With it, all values except for the fixed ones form a so called canonical ensemble, the *Concerted System of Units*.

The program that makes these basic constants and functions available can be found in the appendix. It can also be used in other of my publications. The numerical values calculated with it, in comparison with the corresponding CODATA<sub>2018</sub>-values are shown in Table 1. When preparing the table, I added further values to the system that are simply dependent on



those already defined, including  $\sigma_e$ ,  $a_e$ ,  $g_e$ ,  $\gamma_e$ ,  $\mu_e$ ,  $\mu_N$ ,  $\Phi_0$ ,  $G_0$ ,  $K_J$  and  $R_K$ . Except for  $r_e$ , whose definition is misstated in all editions, I used the expressions and symbols from the CODATA<sub>2018</sub>-document [13] for the other values. Please find the definition of the formula symbols from there.

## 8. Notes to the appendix

The basic formulas and definitions used in this work, are shown in the appendix. It's about the source code for *Mathematica*. The data from the .pdf may be converted into a text file (UTF8), which can be opened directly. Data is presented as a single cell then. However, it is not advantageous to evaluate the entire source code in one single cell. To split, use the Cell/Divide Cell function (*Ctrl/Shift/d*). However, with this procedure there may be problems with special characters, not correctly transferred (e.g.  $\varepsilon$ ,  $\epsilon$ ) or even lead to the conversion being aborted. It is more advantageous to copy and paste data page by page into the text file via clipboard. However, then each line is present as a separate cell. With the command Cell/Merge (*Ctrl/Shift/m*) the cells belonging together can be merged, ideally in blocks between the headings. Then, the values shown in the »Variable« column are available for own calculations.

Symbol	Variable	Calculated (CA)	Source	CODATA <sub>2018</sub> (CD) © COBE Data	$\pm$ Accuracy	$\Delta y$ (CA/CD-1)	Unit
c	c	$2.99792458 \cdot 10^8$	S	$2.99792458 \cdot 10^8$	defined	defined	$m s^{-1}$
$\varepsilon_0$	ep0	$8.854187817620390 \cdot 10^{-12}$	S	$8.854187817620390 \cdot 10^{-12}$	defined	defined	$As V^{-1}m^{-1}$
$\kappa_0$	ka0	$1.369777663190222 \cdot 10^{93}$	S	n.a.	n.a.	defined	$A V^{-1}m^{-1}$
$\mu_0$	my0	$1.256637061435917 \cdot 10^{-6}$	S	$1.256637061435917 \cdot 10^{-6}$	exactly	exactly	$Vs A^{-1}m^{-1}$
k	k	$1.3806485279 \cdot 10^{-23}$	S	$1.380649 \cdot 10^{-23}$	statistic	$+3.41941 \cdot 10^{-7}$	$J K^{-1}$
$\hbar_1$	hb1	$8.795625796565460 \cdot 10^{26}$	S	n.a.	n.a.	defined	$J s$
$\hbar$	hb0	$1.054571817000010 \cdot 10^{-34}$	C	$1.054571817 \cdot 10^{-34}$	defined	$+8.88178 \cdot 10^{-15}$	$J s$
$Q_0$	Q0	$8.340471132242850 \cdot 10^{60}$	C	$8.3415 \cdot 10^{60}$ ©	$3.3742 \cdot 10^{-2}$	$-1.23343 \cdot 10^{-4}$	1
$Z_0$	Z0	376.7303134617700	F	376.73031366857	$1.5 \cdot 10^{-10}$	$-5.48932 \cdot 10^{-10}$	$\Omega$
G	G0	$6.674301499999827 \cdot 10^{-11}$	C	$6.674301499999999 \cdot 10^{-11}$	$2.2 \cdot 10^{-5}$	$-5.48932 \cdot 10^{-10}$	$m^3kg^{-1}s^{-2}$
$G_1$	G1	$9.594550966819210 \cdot 10^{-133}$	C	n.a.	n.a.	unusual	$m^3kg^{-1}s^{-2}$
$G_2$	G2	$1.150360790738584 \cdot 10^{-193}$	F	n.a.	n.a.	unusual	$m^3kg^{-1}s^{-2}$
$m_e/m_p$	mep	$5.446170214846793 \cdot 10^{-4}$	F	$5.4461702148733 \cdot 10^{-4}$	$6.0 \cdot 10^{-11}$	$-4.867 \cdot 10^{-12}$	1
$M_2$	M2	$1.514002834704114 \cdot 10^{114}$	F	n.a.	n.a.	unusual	kg
$M_1$	M1	$1.815248576128075 \cdot 10^{53}$	C	n.a.	n.a.	unusual	kg
$m_p$	mp	$1.6726219236951 \cdot 10^{-27}$	C	$1.6726219236951 \cdot 10^{-27}$	$1.1 \cdot 10^{-5}$	$-2.22045 \cdot 10^{-16}$	kg
$m_e$	me	$9.109383701528 \cdot 10^{-31}$	M	$9.109383701528 \cdot 10^{-31}$	$3.0 \cdot 10^{-10}$	magic $\pm 0$	kg
$m_0$	m0	$2.176434097482374 \cdot 10^{-8}$	C	$2.176434097482336 \cdot 10^{-8}$	calculated	$+1.70974 \cdot 10^{-14}$	kg
$M_H$	MH	$2.609485798792167 \cdot 10^{-69}$	C	n.a.	n.a.	unusual	kg
$T_{p2}$	Tp2	$9.855642915740690 \cdot 10^{153}$	C	n.a.	n.a.	unusual	K
$T_{p1}$	Tp1	$1.181665011421291 \cdot 10^{93}$	C	n.a.	n.a.	unusual	K
$T_{p0}$	Tp0	$1.416784486973613 \cdot 10^{32}$	C	$1.416784486973588 \cdot 10^{32}$	$1.1 \cdot 10^{-5}$	$+1.75415 \cdot 10^{-14}$	K
$T_{k1}$	Tk1	$5.475357175411492 \cdot 10^{152}$	C	n.a.	n.a.	unusual	K
$T_{k0}$	Tk0	2.725436049425770	C	2.72548 ©	$4.3951 \cdot 10^{-5}$	$-1.61258 \cdot 10^{-5}$	K
$r_1$	r1	$1.937846411698606 \cdot 10^{-96}$	F	n.a.	n.a.	unusual	m
$r_0$	r0	$1.616255205549261 \cdot 10^{-35}$	C	$1.616255205549274 \cdot 10^{-35}$	calculated	$-8.21565 \cdot 10^{-15}$	m
$r_e$	re	$2.817940324662071 \cdot 10^{-15}$	C	$2.817940326213 \cdot 10^{-15}$	$4.5 \cdot 10^{-10}$	$-5.50377 \cdot 10^{-10}$	m
$\lambda_C$	$\lambda_{barC}$	$3.861592677230890 \cdot 10^{-13}$	C	$3.861592679612 \cdot 10^{-13}$	$3.0 \cdot 10^{-10}$	$-6.16614 \cdot 10^{-10}$	m
$\lambda_C$	$\lambda_C$	$2.426310237188940 \cdot 10^{-12}$	C	$2.4263102386773 \cdot 10^{-12}$	$3.0 \cdot 10^{-10}$	$-6.13425 \cdot 10^{-10}$	m
$a_0$	a0	$5.291772105440689 \cdot 10^{-11}$	C	$5.291772109038 \cdot 10^{-11}$	$1.5 \cdot 10^{-10}$	$-6.79793 \cdot 10^{-10}$	m
R	R	$1.348032988422084 \cdot 10^{26}$	C	n.a.	at issue	at issue	m
R	RR	4.368617335409830	C	n.a.	at issue	at issue	Gpc

Symbol	Variable	Calculated (CA)	Source	CODATA <sub>2018</sub> (CD) © COBE Data	± Accuracy	Δy (CA/CD-1)	Unit
t <sub>1</sub>	2 t1	6.463959849512312·10 <sup>-105</sup>	F	n.a.	n.a.	unusual	s
t <sub>0</sub>	2 t0	5.391247052483426·10 <sup>-44</sup>	C	5.391247052483470·10 <sup>-44</sup>	calculated	-8.43769·10 <sup>-15</sup>	s
T	2 T	4.496554040802734·10 <sup>17</sup>	C	4.497663485280829·10 <sup>17</sup>	1.1385·10 <sup>-3</sup>	-2.46671·10 <sup>-4</sup>	s
T	2 T	1.424902426903056·10 <sup>10</sup>	C	1.425253996152531·10 <sup>10</sup>	1.1385·10 <sup>-3</sup>	-2.46671·10 <sup>-4</sup>	a
R <sub>∞</sub>	R <sub>∞</sub>	1.097373157632934·10 <sup>7</sup>	C	1.097373156816021·10 <sup>7</sup>	1.9·10 <sup>-12</sup>	+7.44426·10 <sup>-10</sup>	m <sup>-1</sup>
ω <sub>1</sub>	Om1	1.547039312249824·10 <sup>104</sup>	F	n.a.	n.a.	unusual	s <sup>-1</sup>
ω <sub>0</sub>	Om0	1.854858421929227·10 <sup>43</sup>	C	1.854858421929212·10 <sup>43</sup>	calculated	+8.65974·10 <sup>-15</sup>	s <sup>-1</sup>
ω <sub>R∞</sub>	OmR <sub>∞</sub>	2.067068668297942·10 <sup>16</sup>	C	2.067068666759112·10 <sup>16</sup>	1.9·10 <sup>-12</sup>	+7.44451·10 <sup>-10</sup>	s <sup>-1</sup>
cR <sub>∞</sub>	cR <sub>∞</sub>	3.289841962699988·10 <sup>15</sup>	C	3.289841960250864·10 <sup>15</sup>	1.9·10 <sup>-12</sup>	+7.44450·10 <sup>-10</sup>	Hz
H <sub>0</sub>	H0	2.223925234581364·10 <sup>-18</sup>	C	2.223376656062923·10 <sup>-18</sup>	1.1385·10 <sup>-3</sup>	+2.46732·10 <sup>-4</sup>	s <sup>-1</sup>
H <sub>0</sub>	HPC[Q0]	68.62410574852400	C	68.60717815146482←↑©	1.1385·10 <sup>-3</sup>	+2.46732·10 <sup>-4</sup>	kms <sup>-1</sup> Mpc <sup>-1</sup>
q <sub>1</sub>	q1	1.527981474087040·10 <sup>12</sup>	F	n.a.	n.a.	unusual	As
q <sub>0</sub>	q0	5.290817689717126·10 <sup>-19</sup>	C	5.2908176897171 ·10 <sup>-19</sup>	calculated	+4.44089·10 <sup>-15</sup>	As
e	qe	1.602176634000007·10 <sup>-19</sup>	C	1.602176634 ·10 <sup>-19</sup>	exactly	+4.44089·10 <sup>-15</sup>	As
U <sub>1</sub>	U1	8.698608435529670·10 <sup>87</sup>	F	n.a.	n.a.	unusual	V
U <sub>0</sub>	U0	1.042939697003725·10 <sup>27</sup>	C	1.042939697286845·10 <sup>27</sup>	calculated	-2.71463·10 <sup>-10</sup>	V
W <sub>1</sub>	W1	1.360717888312544·10 <sup>131</sup>	F	n.a.	n.a.	unusual	W
W <sub>0</sub>	W0	1.956081416291675·10 <sup>9</sup>	C	1.956081416291641·10 <sup>9</sup>	calculated	+1.73195·10 <sup>-14</sup>	W
S <sub>1</sub>	S1	5.605711433987692·10 <sup>426</sup>	F	n.a.	n.a.	unusual	Wm <sup>-2</sup>
S <sub>0</sub>	S0	1.388921881877266·10 <sup>122</sup>	C	n.a.	n.a.	unusual	Wm <sup>-2</sup>
σ <sub>e</sub>	σe	6.652458724888907·10 <sup>-29</sup>	C	6.6524587321600 ·10 <sup>-29</sup>	9.1·10 <sup>-10</sup>	-1.09299·10 <sup>-9</sup>	m <sup>2</sup>
a <sub>e</sub>	ae	1.159652181281556·10 <sup>-3</sup>	C	1.1596521812818 ·10 <sup>-3</sup>	1.5·10 <sup>-10</sup>	-2.10054·10 <sup>-13</sup>	1
g <sub>e</sub>	ge	-2.00231930436256	C	-2.00231930436256	1.7·10 <sup>-13</sup>	-2.22045·10 <sup>-16</sup>	1
γ <sub>e</sub>	γe	1.760859630228709·10 <sup>11</sup>	C	1.7608596302353 ·10 <sup>11</sup>	3.0·10 <sup>-10</sup>	-3.74278·10 <sup>-12</sup>	s <sup>-1</sup> T <sup>-1</sup>
μ <sub>e</sub>	μe	-9.28476469866128·10 <sup>-24</sup>	C	-9.284764704328 ·10 <sup>-24</sup>	3.0·10 <sup>-10</sup>	-6.10325·10 <sup>-10</sup>	JT <sup>-1</sup>
μ <sub>B</sub>	μB	-9.27401007265130·10 <sup>-24</sup>	C	-9.274010078328 ·10 <sup>-24</sup>	3.0·10 <sup>-10</sup>	-6.12109·10 <sup>-10</sup>	JT <sup>-1</sup>
μ <sub>N</sub>	μN	5.050783742986264·10 <sup>-27</sup>	C	5.0507837461150 ·10 <sup>-27</sup>	3.1·10 <sup>-10</sup>	-6.19456·10 <sup>-10</sup>	JT <sup>-1</sup>
Φ <sub>0</sub>	Φ0	2.067833847194937·10 <sup>-15</sup>	C	2.067833848 ..... ·10 <sup>-15</sup>	exactly	-3.89327·10 <sup>-10</sup>	Wb
G <sub>0</sub>	GQ0	7.748091734611053·10 <sup>-5</sup>	C	7.748091729000002·10 <sup>-5</sup>	exactly	+7.24185·10 <sup>-10</sup>	S
K <sub>J</sub>	KJ	4.835978487132911·10 <sup>14</sup>	C	4.835978484 ..... ·10 <sup>14</sup>	exactly	+6.47834·10 <sup>-10</sup>	HzV <sup>-1</sup>
R <sub>K</sub>	RK	2.581280744348851·10 <sup>4</sup>	C	2.581280745 ..... ·10 <sup>4</sup>	exactly	-2.52258·10 <sup>-10</sup>	Ω
α	alpha	7.297352569776440·10 <sup>-3</sup>	F	7.297352569311 ·10 <sup>-3</sup>	1.5·10 <sup>-10</sup>	+6.37821·10 <sup>-11</sup>	1
δ	delta	9.378551014802563·10 <sup>-1</sup>	F	9.378551009654370·10 <sup>-1</sup>	1.5·10 <sup>-10</sup>	+5.48932·10 <sup>-10</sup>	1
χ̄	xtilde	2.821439372122070	F	2.821439372 .....	exactly	exactly	1
σ	σ	5.670366673885495·10 <sup>-8</sup>	C	5.670366673885496·10 <sup>-8</sup>	exactly	exactly	Wm <sup>-2</sup> K <sup>-4</sup>

S Subspace value (const)  
F Fixed value (invariable)

M Magic value  
C Calculated (calculated)

MachinePrecision → ±2.22045·10<sup>-16</sup>

Table 1:  
Concerted International  
System of Units

## 9. References

- [ 1] **Gerd Pommerenke**  
The Shape of the Universe, Augsburg 2021 (2005-2013, 2020-2021) *viXra:1310.0189*  
6th revised edition, please update older editions + *[Corrigendum]* *viXra:2203.0090*
- [ 2] **H.-J. Treder** (Herausgeber), Gravitationstheorie und Theorie der Elementarteilchen,  
Wiederabdruck ausgewählter Beiträge des Einstein-Symposiums 1965 in Berlin  
**Cornelius Lanczos**†, *Dublin, Irland*,  
»Tetraden-Formalismus und definite Raum-Zeit-Struktur«,  
Akademieverlag, Berlin (O) 1979, S. 24 ff. (German)  
ISBN: none, Lizenznummer:202 • 100/559/78, Bestellnummer: 762 6051 (6506) • LSV 111,  
Alternative source German: *viXra:1906.0321* pp. 9-15  
Alternative source English: *viXra:1310.0189* pp. 9-15
- [ 3] **Prof. Dr. sc. techn. Dr. techn. h.c. Eugen Philippow**, TH Ilmenau  
Taschenbuch der Elektrotechnik, Band 2, Grundlagen der Informationstechnik  
Verlag Technik Berlin, 1. Auflage 1977  
ASIN: B008365UYE
- [ 4] **Slater/Lucy/Joan**, Generalized Hypergeometric Functions,  
Cambridge 1966  
ISBN:978-0521090612
- [ 5] **Bronstein†/Semendjajew**, Taschenbuch der Mathematik  
BSB B. G. Teubner Verlagsgesellschaft, Leipzig 1979  
ISBN: 3322004740
- [ 6] **Sieber/Sebastian**, Spezielle Funktionen,  
Mathematik für Ingenieure, Naturwissenschaftler, Ökonomen und Landwirte,  
Band 12, BSB B. G. Teubner Verlagsgesellschaft, Leipzig 1977  
ISBN: none, VLN: 294-375/47/77 • LSV 1034, Bestellnummer: 6657980
- [ 7] **Brockhaus ABC Physik**,  
F.A. Brockhaus-Verlag Leipzig 1972
- [ 8] **Gernot Neugebauer**, Relativistische Thermodynamik,  
Akademieverlag, Berlin (O) 1980  
ISBN: 978-3528068639
- [ 9] **Gerd Pommerenke**  
The Metric Universe, 3<sup>rd</sup> edition, Augsburg 2024, *viXra:2209.0026* and  
[10.13140/RG.2.2.27826.48324/2](https://doi.org/10.13140/RG.2.2.27826.48324/2)
- [10] **Gerd Pommerenke**  
The Electron and Weak Points of the Metric System,  
2nd edition, Augsburg 2023, *viXra:2201.0122* and  
[10.13140/RG.2.2.32859.64801/2](https://doi.org/10.13140/RG.2.2.32859.64801/2)
- [11] **Pereira MA (2016)**  
The Hypergeometrical Universe: Cosmogenesis, Cosmology and Standard Model.  
J Generalized Lie Theory Appl 10:248.  
<https://doi.org/10.4172/1736-4337.1000248>
- [12] **User Geek3: Datei „VFpt charges plus minus.svg“**. In: Wikimedia Commons,  
Bearbeitungsstand: Mai 2010. Bilddatei wurde nachbearbeitet und ergänzt gemäß  
Creative Commons Attribution-Share Alike 3.0 Unported license ©:  
[https://commons.wikimedia.org/wiki/File:VFpt\\_charges\\_plus\\_minus.svg](https://commons.wikimedia.org/wiki/File:VFpt_charges_plus_minus.svg)  
(Abgerufen: 25. März 2023, 10:28 UTC)
- [13] **Fundamental Physical Constants –Extensive Listing**,  
In: 2018 CODATA adjustment  
<https://physics.nist.gov/cgi-bin/cuu/Category?view=pdf&All+values.x=64&All+values.y=13>

# The Concerted International System of Units

## Declarations

```
Off[General::spell]
Off[General::spell1]
Off[InterpolatingFunction::dmval]
Off[FindMaximum::lstol]
Off[FindRoot::nlnum]
```

## Units

```
km = 1000;
pc = 3.08572*10^16;
Mpc = 3.08572*10^19 km;
minute = 60;
hour = 60 minute;
day = 24*hour;
year = 365.24219879*day;
F0 = 2.51*10^-8 (*Zero flux brightness Wm^-2*);
L0 = 3.09*10^28 (*Zero luminosity W*);
L1a= 6.40949*10^35 (*Standard candle SNIa W*);
```

## Basic Values

```
c=2.99792458*10^8; (*Speed of light*);
my0=4 Pi 10^-7; (*Permeability of vacuum*);
ka0=1.3697776631902217*10^93; (*Conductivity of vacuum*);
hb1=8.795625796565464*10^26; (*Planck constant slashed init*);
k=1.3806485279*10^-23; (*Boltzmann constant*);
me=9.109383701528*10^-31; (*Electron rest mass with Q0 Magic value 1*);
mp=1.6726219236951*10^-27; (*Proton rest mass Magic value 2*);
```

## Auxilliary Values

```
mep=SetPrecision[me/mp,20]; (*Mass ratio e/p*);
ma=1822.8884862171988 me; (*Atomic mass unit*);
ε=ArcSin[0.3028221208819742993334500624769134447]-3Pi/4; (*RnB angle ε null(fix)*);
γ=Pi/4-ε; (*RnB angle γ nullvector*);
ζ=1/(36Pi^3)(3Sqrt[2])^(-1/3)/mep; (*re-correction factor*);
xtilde=xtilde=3+N[ProductLog[-3E^-3]]; (*Wien displacement law constant (v)*);
alpha=Sin[Pi/4-[Epsilon]]^2/(4Pi); (*Correction factor QED \[Alpha](Q0)*);
delta=4Pi/alpha*mep; (*Correction factor QED \[Delta](Q0)*);
(*Q0=(9Pi^2 Sqrt[2]delta me/my0/ka0/hb0SI)^(-3/4) (*Phase Q0=2ω0t during calibration*);*)
Q0=(9 Pi^2 Sqrt[2]delta me/my0/ka0/hb1)^(-3/7); (*Phase Q0=2ω0t after calibration*);
```

## Composed Expressions

```
Z0=my0 c; (*Field wave impedance of vacuum*);
ep0=1/(my0 c^2) (* Permittivity of vacuum*);
R∞=1/(72 Pi^3)/r1 Sqrt[2] alpha^2 /delta Q0^(-4/3); (*Rydberg constant*);
Oml=ka0/ep0; (*Cutoff frequency of subspace*);
Om0=Oml/Q0; (*Planck's frequency*);
OmR∞=2 Pi c R∞; (*Rydberg angular frequency*);
cR∞=c R∞; (*Rydberg frequency*);
H0=Om1/Q0^2; (*Hubble parameter local*);
H1=3/2*H0; (*Hubble parameter whole universe*);
r1=1/(ka0 Z0); (*Planck's length subspace*);
a0=9Pi^2 r1 Sqrt[2] delta/alpha Q0^(4/3); (*Bohr radius*);
λbarC=a0 alpha; (*Reduced Compton wavelength*);
λC=2 Pi λbarC; (*Compton wavelength electron*);
re= r1 (2/3)^(1/3)/ζ Q0^(4/3); (*Classic electron radius*);
r0= r1 Q0; (*Planck's length vac*);
R= r1 Q0^2; (*World radius*);
RR=R/Mpc/1000; (*World radius Gpc*);
t1=1/(2 Om1); (*Planck time subspace*);
t0=1/(2 Om0); (*Planck time vacuum*);
T=1/(2 H0); (*World time constant*);
TT=2T/year; (*The Age*);
hb0=hb1/Q0; (*Planck constant slashed*);
h0=2Pi*hb0; (*Planck constant unslashed*);
q1=Sqrt[hb1/Z0]; (*Universe charge*);
q0=Sqrt[hb1/Q0/Z0]; (*or qe/Sin[π/4-ε] Planck charge*);
qe=q0 Sin[Pi/4-ε]; (*Elementary charge e*);
M2=my0 ka0 hb1; (*Total mass with Q=1*);
```

```

M1=M2/Q0;
m0=M2/Q0^2;
(*m0=(9Pi^2Sqrt[2]*delta*me)^.75*(my0*ka0*hb0SI)^.25;
mp=4Pi me/alpha/delta;
(*me=Sqrt[hb1/Q0/Z0]*Sin[Pi/4-ε];
MH=M2/Q0^3;
G0=c^2*r0/m0; (*hb0*c/m0^2*);
G1=G0/Q0^2;
G2=G0/Q0^3;
U0=Sqrt[c^4/4/Pi/ep0/G0];
U1=U0*Q0;
W1=Sqrt[hb1 c^5/G2];
W0=W1/Q0^2;
S1=hb1 Om1^2/r1^2;
S0=S1/Q0^5;
Sk1=4Pi^2*E^2/18^4/60*hb1*Om1^2/r1^2;
Sk0=Sk1/Q0^4/Q0^3/E^2;
wk1=Sk1/c ;
wk0=Sk0/c ;
Wk1=wk1*r1^3;
μB=-9/2Pi^2 Sqrt[2 hb1/Z0]delta Sin[γ]/my0/ka0 Q0^(5/6);
μN=-μB*mep;
μe=1.0011596521812818 μB
Tk1=hb1 Om1/18/k;
Tk0=Tk1/Q0^(5/2);
Tp0=Sqrt[hb0 c^5/G0]/k; Tp1=Tp0*Q0; Tp2=Tp0*Q0^2;
φ0=Pi Sqrt[hb1 Z0/Q0 ]/Sin[Pi/4-ε];
GQ0=1/Pi/Z0*Sin[Pi/4-ε]^2;
KJ=2q0 Sin[Pi/4-ε]/h0;
RK=.5 my0 c/alpha;
σe=8Pi/3 re^2;
ae=SetPrecision[μe/μB,20]-1;
ge=-2(1+ae);
ye=2 Q0 Abs[μe]/hb1;
σ1= SetPrecision[Pi^2/60 k^4/c^2/hb1^3, 16];
σ=σ1*Q0^3;
(*Mach mass*);
(*Planck mass downwardly*);
(*Planck mass upwardly*);
(*Proton rest mass with Q0*);
(*if using Q0 as Magic value*);
(*Hubble mass*);
(*Gravity constant local*);
(*Gravity constant Mach*);
(*Gravity constant Init*);
(*Planck voltage generic*);
(*Planck voltage Mach*);
(*Energy with Q=1*);
(*Planck energy*);
(*Poynting vector metric with Q=1*);
(*Poynting vector metric actual*);
(*Poyntingvec CMBR initial*);
(*Poyntingvec CMBR actual*);
(*Energy density CMBR initial*);
(*Energy density CMBR actual*);
(*Energy CMBR initial*);
(*Bohr magneton*);
(*Nuclear magneton*);
(*Electron magnetic moment*);
(*CMBR-temperature Q=1*);
(*CMBR-temperature*);
(*Planck-temperature*);
(*Magnetic flux quantum Pi h/e*);
(*Conductance quantum e^2/Pi h*);
(*Josephson constant 2e/h*);
(*von Klitzing constant μ0c/2α*);
(*Thomson cross section (8Pi/3)re^2*);
(*Electron magnetic moment anomaly*);
(*electron g-factor*);
(*electron gyromagnetic ratio*);
(*Stefan-Boltzmann constant initial*);
(*Stefan-Boltzmann constant*);

```

### Basic Functions

```

cMc=Function[-2 I/#/Sqrt[1-(HankelH1[2,#]/HankelH1[0,#])^2]];
Qr=Function[#1/Q0/2/#2];
PhiQ=Function[If[##>10^4,-Pi/4-3/4/#,
Arg[1/Sqrt[1-(HankelH1[2,#]/HankelH1[0,#])^2]]-Pi/2]]; (*Angle of c arg θ(Q)*);
PhiR=Function[PhiQ[Qr[#1,#2]]];
RhoQ=Function[If[##<10^4,N[2/#/Abs[Sqrt[1-
HankelH1[2,#]/HankelH1[0,#])^2]],1/Sqrt[##]];
RhoR=Function[RhoQ[Qr[#1,#2]]];
AlphaQ=Function[Pi/4-PhiQ[#]]; (*Angle α*);
AlphaR=Function[N[Pi/4-PhiR[#1,#2]]];
BetaQ=Function[Sqrt[#1]*((#2)^2+#1^2*(1-(#2)^2)^(-.25)];
GammaPQ=Function[N[PhiQ[#]+ArcCos[RhoQ[#]*Sin[AlphaQ[#]]]+Pi/4]];
HPC=Function[Om1/#^2/km*Mpc]; (*H0=f(Q0)[km*s-1*Mpc-1]*);
rq={{0,0}};
For[x=-8;i=0,x<4,++i,x+=.01;AppendTo[rq,{10^x,N[10^x*RhoQ[10^x]]}]];
RhoQ1=Interpolation[rq];
RhoQQ1=Function[If[##<10^3,RhoQ1[#],Sqrt[##]]; (*Interpolation RhoQ*);
Rk=Function[If[##<10^5,3/2*Sqrt[#]*NIntegrate[RhoQQ1[x],{x,0,#}],6#]];
Rn=Function[Abs[3/2*Sqrt[#]*NIntegrate[RhoQQ1[x]*Exp[I*(PhiQ[x])],{x,0,#}]]];
RnB=Function[Arg[NIntegrate[RhoQQ1[x]*Exp[I*(PhiQ[x])],{x,0,#}]]];
alphaF=Function[Sin[Pi/2+ε-(RnBP)*RnB[#]]^2/(4Pi)]; (*RnBP def further below*);
deltaF=Function[4Pi/alphaF[#]*mep]; (*Correction factor QED ΔQ*);

```

### End of Metric System Definition

```

rn={};
For[d=-6.01; i=0,d<6.01,++i,d+=.05; AppendTo[rn,{d,RnB[10^d]/Pi}]]
RnB1=Interpolation[rn]; (*RnB angle ε nullvector from Q*);
RnB=Function[If[##<10^-8,Null,If[##<10^6,RnB1[Log10[#]],-.25]]];
RnBP=Function[If[##<10^-8,Null,If[##<10^6,Pi RnB1[Log10[#]],-Pi/4]]];
alphaF=Function[Sin[Pi/2+ε-RnBP[#]]^2/(4Pi)]; (*Redfinition for faster calculation*);

```

### End of Optional Metric System Definition